OAK RIDGE NATIONAL LABORATORY LIBRARIES
3 4456 0548422 2

CENTRAL RESEARCH LIBRARY

ORNL-5174

Cy 1

Effect of Long-Term Aging at 815° C on the Tensile Properties and Microstructural Stability of Four Cobalt- and Nickel-Base Superalloys

J. P. Hammond

OAK RIDGE NATIONAL LABORATORY
CENTRAL RESEARCH LIBRARY
DOCUMENT COLLECTION
LIBRARY LOAN COPY
DO NOT TRANSFER TO ANOTHER PERSON
If you wish someone else to see this document, send in name with document and the library will arrange a loan.
UCN-7969
(3 3-67)

OAK RIDGE NATIONAL LABORATORY
OPERATED BY UNION CARBIDE CORPORATION FOR THE ENERGY RESEARCH AND DEVELOPMENT ADMINISTRATION

Printed in the United States of America. Available from
National Technical Information Service
U.S. Department of Commerce
5285 Port Royal Road, Springfield, Virginia 22161
Price: Printed Copy $4.00; Microfiche $2.25

This report was prepared as an account of work sponsored by the United States Government. Neither the United States nor the Energy Research and Development Administration/United States Nuclear Regulatory Commission, nor any of their employees, nor any of their contractors, subcontractors, or their employees, makes any warranty, express or implied, or assumes any legal liability or responsibility for the accuracy, completeness or usefulness of any information, apparatus, product or process disclosed, or represents that its use would not infringe privately owned rights.

ORNL-5174
UC-33 (Nuclear
Propulsion Systems
and Aerospace Safety)

Contract No. W-7405-eng-26

METALS AND CERAMICS DIVISION

EFFECT OF LONG-TERM AGING AT 815°C ON THE TENSILE PROPERTIES AND MICROSTRUCTURAL STABILITY OF FOUR COBALT- AND NICKEL-BASE SUPERALLOYS

J. P. Hammond

AUGUST 1976

OAK RIDGE NATIONAL LABORATORY
Oak Ridge, Tennessee 37830
operated by
UNION CARBIDE CORPORATION
for the
ENERGY RESEARCH AND DEVELOPMENT ADMINISTRATION

OAK RIDGE NATIONAL LABORATORY LIBRARIES
3 4456 0548422 2

CONTENTS

ABSTRACT 1
INTRODUCTION 1
MATERIALS AND METHODS 2
RESULTS 3
Tensile Tests 3
Metallographic and Electron-Beam Scanning Examinations . . . 10
Phase Identifications 23
DISCUSSION OF RESULTS 26
SUMMARY AND CONCLUSIONS 29
ACKNOWLEDGMENTS 30

EFFECT OF LONG-TERM AGING AT 815°C ON THE TENSILE PROPERTIES AND MICROSTRUCTURAL STABILITY OF FOUR COBALT- AND NICKEL-BASE SUPERALLOYS

J. P. Hammond

ABSTRACT

Two heats of Haynes alloy 25 and one heat each of Haynes alloy 188, Hastelloy N, and Inconel 625 were tensile tested after aging for 11,000 hr at 816°C (1500°F). Yield strength, ultimate tensile strength, and elongation were determined 24, 316, 760, and 982°C (75, 600, 1400, and 1800°F) and compared with typical properties for these materials in the solution annealed condition. Toughness values were determined for these materials from their engineering stress-strain curves. The long-term aging treatment degraded ductility and toughness at room temperature but, contrary to behavior expected for overaging, enhanced them over those for the solution annealed condition in tests at 760°C. The tensile properties of the aged superalloys were correlated with mode of fracture and the amounts, identity, and morphology of the precipitates. Aging substantially depleted the hardener tungsten from the matrix in the cobalt-base alloys.

INTRODUCTION

Among several criteria for evaluating containment materials for isotopic power conversion applications are good mechanical properties and their retention with thermal aging. Degradation of toughness and ductility, promoted by microstructural instability and precipitation of embrittling carbides and/or intermetallic compounds, is of special concern in cobalt- and nickel-base superalloys.

In an earlier materials evaluation study conducted for the Division of Space Nuclear Systems, U.S. Atomic Energy Commission[1] by the Hittman Corporation, Maryland, for space power applications, tensile specimens of a number of superalloys presently of interest for power conversion units for earth-bound applications were aged for a very long period (around 11,000 hr) at the temperature at which embrittling phases are

---

[1]Succeeded by the Division of Nuclear Research and Applications, Energy Research and Development Administration.

most prone to precipitate (815°C). However, these specimens were never tested by Hittman and ultimately were shipped to ORNL for tests. Room- and elevated-temperature tensile tests, coupled with correlative analytical examinations, were made of the specimens. Since materials in the same heats were not available in the solution annealed condition, typical tensile properties for this condition obtained from vendors were employed for assessing degradation of properties with aging.

MATERIALS AND METHODS

The alloys tested included two heats Haynes alloy 25 (0.36% Si and 0.01% Si), Haynes alloy 188, Hastelloy N, and Inconel 625. The alloys in the product forms tested [0.7 to 1.8-mm (0.025 to 0.070-in.) sheet] were supplied by the Cabot Corporation and International Nickel Company from regular production heats. Strip tensile specimens with a gage section 25.4 mm long by 6.3 mm wide (1 by 0.25 in.) were machined from sheet stock and subsequently solution annealed. These were then encapsulated in quartz tubing and aged in vacuum of 1 mPa (10^{-5} torr) at 815 ± 5°C. Finally, the specimens were cleaned by the DS-9 brightening process.[2] The vendors' chemical analyses and heat numbers of the alloys are given in Table 1.

[2]Proprietary process of Diversey Chemical Company, Des Plaines, Illinois.

Table 1. Chemical Analyses of Superalloys

Element	Content, wt %, for Each Alloy (Heat)				
	Haynes 25 (B18509)	Haynes 25 (186-6-1816)	Haynes 188 (8188-7-0124)	Inconel 625 (10x24A8As)	Hastelloy N (284-4-5109)
Co	Bal	Bal	Bal		0.11
Ni	10.59	9.25	21.44	62.05	Bal
Cr	20.18	19.77	22.27	21.66	6.96
Fe	1.58	2.02	1.33	2.97	3.67
Y					0.26
Mo				8.98	16.50
W	14.66	14.42	14.49		0.26
Nb + Ta				3.54	
Al + Ti					0.13
Al				0.17	
Ti				0.29	
Cu				0.01	0.01
Mn	1.70	1.33	0.76	0.01	0.56
B					0.008
C	0.078	0.10	0.11	0.04	0.06
Si	0.36	0.01	0.08	0.25	0.70
P	0.010	0.020	0.012		0.001
S	0.010	0.007	0.001	0.007	0.008
La			0.04		

Tensile tests were conducted in duplicate on the aged specimens at 24, 316, 760, and 982°C on an Instron testing machine at a strain rate (crosshead) of 0.05 in./min in air. The test temperature was controlled to ±2°C. Optical microstructural examinations and electron-beam scans of fracture surfaces were made on the aged tensile specimens after testing at 24 and 760°C for correlation with the test results. These particular test temperatures were selected for study because of the contrast in properties obtained at them. Whereas the phases that precipitate with aging at 815°C had been identified in the cobalt-base alloys, we identified prominent phases for the specific aging period to aid the rationalization of results. This was accomplished by electrolytic extraction and analysis of residues by x-ray diffraction. The separations were accomplished with an electrolyte of 10% concentrated HCl in methanol, and the diffraction patterns of phases were developed on a Norelco diffractometer.

RESULTS

Tensile Tests

The complete results of the tensile tests conducted on aged alloys along with typical results for the solution-annealed condition are presented in Table 2. Composite graphs comparing yield strength (YS), ultimate tensile strength (UTS), and total elongation (TE) of the individual alloys (solution-annealed and aged) as functions of temperature are given in Figs. 1 through 4, and graphs of these separate properties for all the alloys together are given in Figs. 5 through 7. To compare toughnesses displayed in the individual tensile tests, energies of deformation incurred at the points of ultimate stress and fracture stress were established by determining areas under the engineering stress-strain curves by the Johnson integration method. The energy values in duplicate for the various alloys and test temperatures are recorded in Table 2, whereas bar charts of averaged values are presented in Fig. 8 to facilitate comparisons.

An assessment of mechanical properties (YS, UTS, and TE) of the alloys shows that except for the tensile strength of Hastelloy N (Fig. 3) and yield strength of Inconel 625 (Fig. 4), the two strength properties are not very significantly altered by aging. On the other hand, total elongation through the complete temperature span is dramatically changed. At room temperature, the ductility was reduced by amounts that ranged from 33% (for Inconel 625) to as much as 86% (0.36% Si Haynes alloy 25). The yield strength of Inconel 625 increased by 27 to 30% over the temperature range from 24 to 760°C (Fig. 5). The combined high yield strength and ductility noted for Inconel 625 at 24°C suggests high room-temperature fracture toughness, and, as will be shown subsequently, it proved to be the highest by far of all alloys tested at 24°C.

In the solution-annealed condition, pronounced minima were exhibited in the percent elongation curves for each of the alloys at around 760°C (see Figs. 1–4 or 7). At approximately the same general temperature,

Table 2. Tensile Properties of Alloys After Long-Time Aging at 816°C (1500°F) Compared with Solution Annealed Material

Aging Time (hr)	Temperature (°C)	Temperature (°F)	Stress, MPa (ksi) Yield (0.2%)	Stress, MPa (ksi) Ultimate Tensile	Stress, MPa (ksi) Fracture	Strain, % Total	Strain, % Uniform	Deformation Energy, J (ft-lb) At Ultimate	Deformation Energy, J (ft-lb) At Fracture
Haynes Alloy 25 [0.36% Si, 1.52-mm (0.060-in.) Sheet][a]									
0	24	75	448 (65)	931 (135)		60			
11,448	24	75	427 (61.9)	821 (119.1)	821 (119.1)	7.9	7.9	1063 (784)	1063 (784)
11,448	24	75	426 (61.8)	847 (122.9)	847 (122.9)	8.8	8.8	1205 (889)	1205 (889)
0	316	600	305 (44.3)	830 (120.4)		80			
11,448	316	600	316 (45.9)	771 (111.8)	771 (111.8)	20.0	20.0	2278 (1680)	2278 (1680)
11,448	316	600	304 (44.1)	760 (110.2)	760 (110.2)	18.3	18.3	2037 (1503)	2037 (1503)
0	760	1400	242 (35.1)	583 (84.5)		28			
11,448	760	1400	242 (35.1)	550 (79.8)	461 (66.9)	53.1	20.0	1686 (1243)	4400 (3245)
11,448	760	1400	254 (36.8)	560 (81.3)	465 (67.4)	53.0	18.4	1839 (1356)	4704 (3469)
0	982	1800	126 (18.2)	231 (33.5)		40			
11,448	982	1800	152 (22.0)	182 (26.4)	114 (16.6)	48.0	6.0	186 (137)	1248 (921)
Haynes Alloy 25 [0.01% Si, 1.65-mm (0.065-in.) Sheet][a]									
0	24	75	448 (65.0)	931 (135.0)		60			
11,448	24	75	398 (57.8)	927 (134.5)	927 (134.5)	10.2	10.2	1453 (1072)	1453 (1072)
11,448	24	75	380 (55.1)	1022 (148.3)	1022 (148.3)	10.8	10.8	1511 (1115)	1511 (1115)
0	316	600	305 (44.3)	830 (120.4)		80			
11,448	316	600	329 (47.7)	823 (119.4)	823 (119.4)	20.2	20.2	2450 (1807)	2450 (1807)
11,448	316	600	327 (47.4)	767 (111.2)	767 (111.2)	13.8	13.8	1670 (1231)	1670 (1231)
0	760	1400	242 (35.1)	583 (84.5)		28			
11,448	760	1400	262 (38.0)	586 (85.0)	475 (68.9)	57.7	16.7	1518 (1120)	5029 (3709)
11,448	760	1400	261 (37.8)	584 (84.7)	463 (67.2)	59.4	16.6	1518 (1120)	5121 (3777)
0	982	1800	126 (18.2)	231 (33.5)		40			
11,448	982	1800	152 (22.0)	182 (26.4)	114 (16.6)	48.1	6.0		
11,448	982	1800	73 (10.6)	92 (13.4)	27 (3.9)	75.0	7.7	177 (131)	1766 (1303)
Haynes Alloy 188 [0.08% Si, 1.32-mm (0.052-in.) Sheet][b]									
0	24	75	479 (69.5)	961 (139.4)		56			
10,998	24	75	452 (65.6)	952 (138.0)	952 (138.0)	14.1	14.1	2084 (1537)	2084 (1537)
10,998	24	75	465 (67.4)	964 (139.8)	964 (139.8)	14.8	14.8	2228 (1644)	2228 (1644)
0	316	600	334 (48.5)	802 (116.3)		71			
10,998	316	600	331 (48.0)	804 (116.6)	804 (116.6)	19.5	19.5	2335 (1722)	2335 (1722)
10,656	316	600	359 (52.1)	877 (127.2)	877 (127.2)	20.1	20.1	2684 (1979)	2684 (1979)
0	760	1400	291 (42.2)	634 (92.0)		43			
10,656	760	1400	274 (39.7)	497 (72.1)	384 (55.7)	56.8	22.1	1021 (753)	4150 (3061)
10,656	760	1400	281 (40.8)	512 (74.2)	511 (74.1)	63.3	13.3	1072 (791)	4654 (3432)
0	982	1800	162 (23.5)	254 (36.8)		72			
10,656	982	1800	90 (13.1)	105 (15.2)	25 (3.6)	54.9	6.3	165 (121)	1147 (846)
10,656	982	1800	232 (33.7)	291 (42.2)	90 (13.0)	57.6	7.9	351 (259)	2321 (1712)

Table 2. (Continued)

Aging Time (hr)	Temperature (°C)	Temperature (°F)	Stress, MPa (ksi) Yield (0.2%)	Stress, MPa (ksi) Ultimate Tensile	Stress, MPa (ksi) Fracture	Strain, % Total	Strain, % Uniform	Deformation Energy, J (ft-lb) At Ultimate	Deformation Energy, J (ft-lb) At Fracture
				Hastelloy N [0.66-mm (0.0026-in.) Sheet]					
0[c]	24	75	308 (44.7)	789 (114.4)		50			
10,968	24	75	336 (48.7)	631 (91.5)	631 (91.5)	13.6	13.6	1267 (934)	1267 (934)
10,968	24	75	341 (49.5)	641 (93.0)	641 (93.0)	15.3	15.3	1429 (1054)	1429 (1054)
0[d]	316	600	248 (36.0)	712 (103.3)		55			
10,968	316	600	251 (36.4)	585 (84.9)	585 (84.9)	19.9	19.9	1684 (1242)	1684 (1242)
10,656	316	600	253 (36.7)	603 (87.5)	592 (85.8)	22.6	22.2	1886 (1391)	1915 (1412)
0[c]	760	1400	181 (26.2)	426 (61.8)		21			
10,656	760	1400	210 (30.4)	441 (63.9)	427 (61.9)	20.5	15.7	974 (718)	1309 (965)
10,656	760	1400	210 (30.4)	439 (63.7)	418 (60.6)	22.2	15.9	989 (729)	1431 (1055)
0[d]	982	1800	138 (20.0)	140 (20.3)		28.4			
10,656	982	1800	136 (19.7)	138 (20.0)	62 (9.0)	61.3	1.9	50.2 (37.0)	1089 (803)
10,656	982	1800	133 (19.3)	139 (20.1)	74 (10.8)	62.9	2.5	62.1 (45.8)	1125 (830)
				Inconel 625 [1.78-mm (0.070-in.) Sheet][e]					
0	24	75	428 (62)	934 (135.5)		51			
10,656	24	75	530 (76.8)	955 (138.5)	955 (138.5)	34.8	34.8	4431 (3268)	4431 (3268)
10,656	24	75	578 (83.9)	974 (141.3)	974 (141.3)	33.5	33.5	4992 (3682)	4992 (3682)
0	316	600	331 (48)	838 (121.5)		52			
10,656	316	600	443 (64.3)	854 (123.8)	854 (123.8)	25.0	25.0	2978 (2197)	2978 (2197)
10,656	316	600	478 (69.4)	870 (126.2)	870 (124.4)	21.7	21.5	2823 (2082)	2823 (2082)
0	760	1400	307 (44.5)	620 (90)		68			
10,656	760	1400	388 (56.2)	482 (69.9)	208 (30.2)	60.0	5.5	5022 (371)	4083 (3012)
10,656	760	1400	389 (56.4)	484 (70.2)	194 (28.2)	70.0	5.2	481 (354)	4259 (3141)
0	982	1800	141 (20.5)	141 (20.5)		117			
10,968	982	1800	105 (15.2)	111 (16.1)	0 (0.0)	130.0	1.9	43.4 (32.0)	1262 (930)
10,968	982	1800	104 (15.1)	110 (15.9)	21 (3.0)	97.8	2.3	52.5 (38.7)	1338 (987)

[a]Values for unaged material are typical values by Cabot for solution annealed 2.77-mm (0.109-in.) sheet.

[b]Values for unaged material are typical values by Cabot for solution annealed 0.76- to 1.65-mm (0.030–0.065-in.) sheet.

[c]Typical values by Cabot for solution annealed 1.14-mm (0.045-in.) sheet.

[d]Average of ORNL values for 6.4-mm-diam (0.25-in.) specimens of two heats.

[e]Values for unaged material are typical values by INCO for 1.57-mm (0.062-in.) sheet.

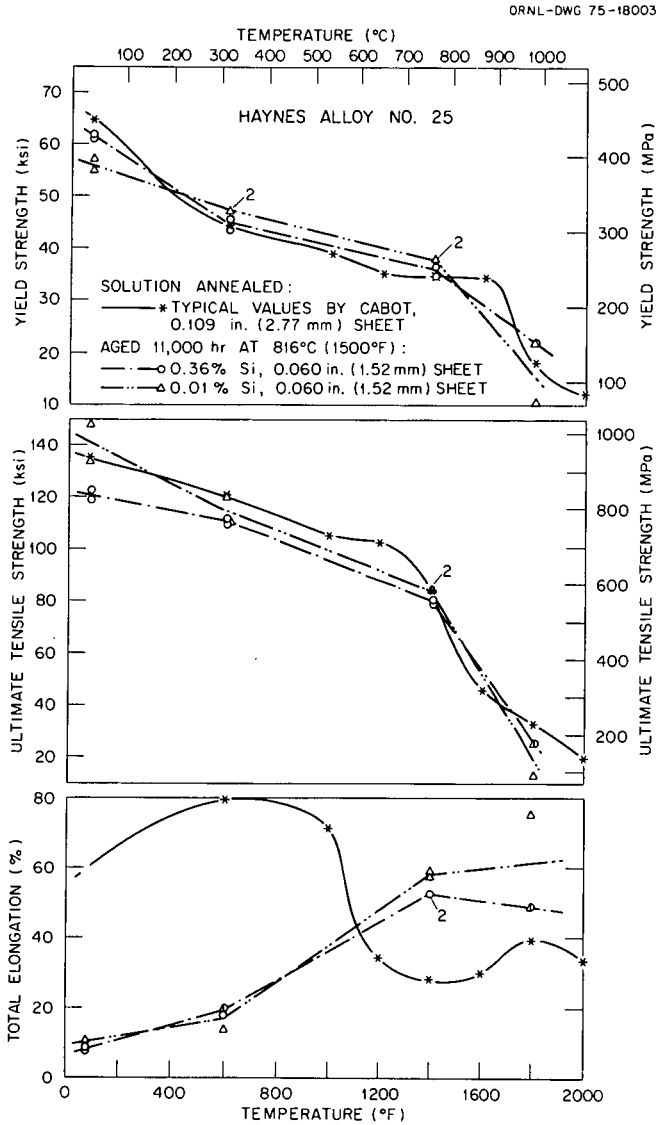

Fig. 1. Comparisons Between Effects of Solution Annealed and Aged Conditions on the Yield Strength, Ultimate Tensile Strength, and Total Elongation of Haynes Alloy 25.

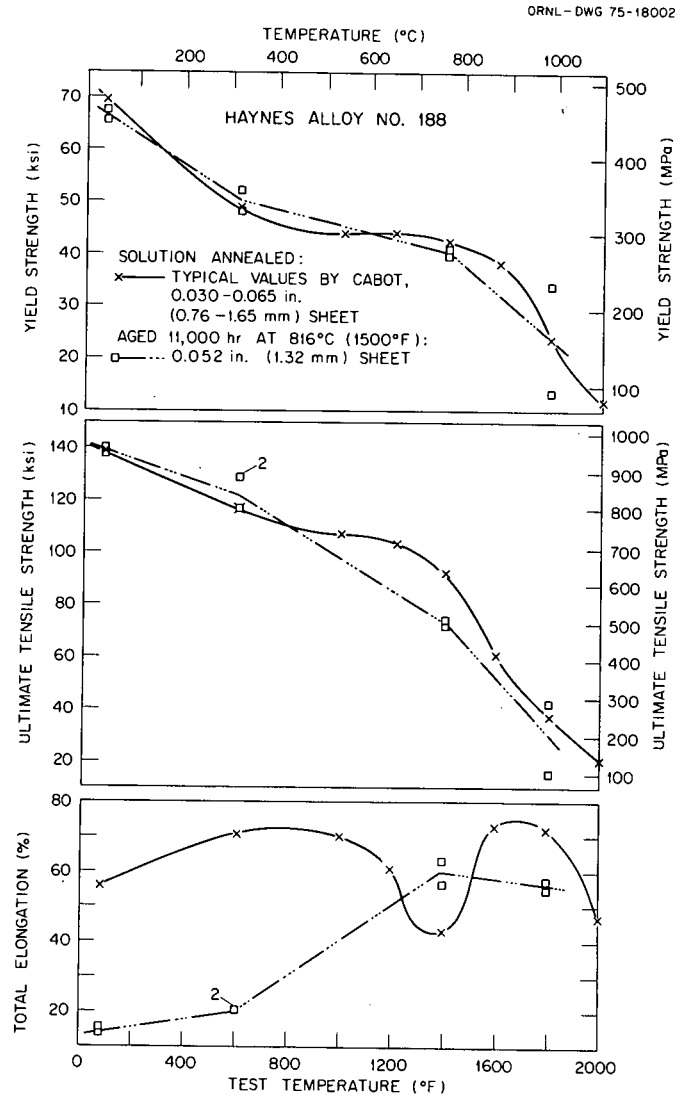

Fig. 2. Comparisons Between Effects of Solution Annealed and Aged Conditions on the Yield Strength, Ultimate Tensile Strength, and Total Elongation of Haynes Alloy 188.

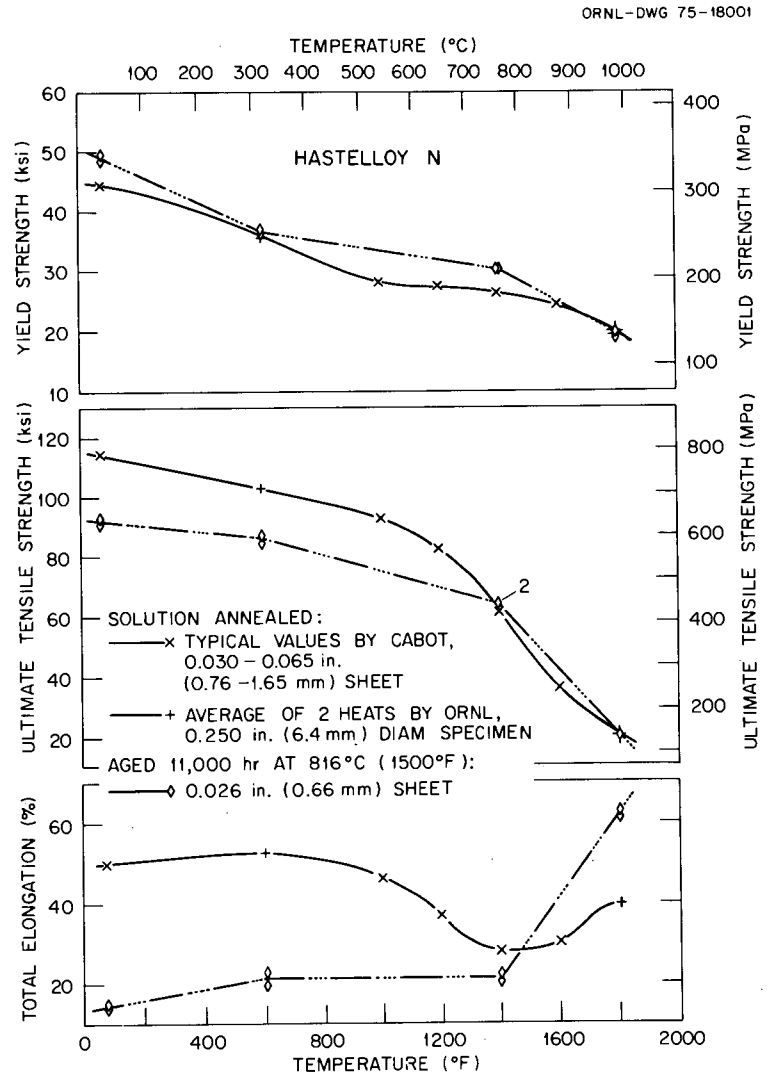

Fig. 3. Comparisons Between Effects of Solution Annealed and Aged Conditions on the Yield Strength, Ultimate Tensile Strength, and Total Elongation of Hastelloy N.

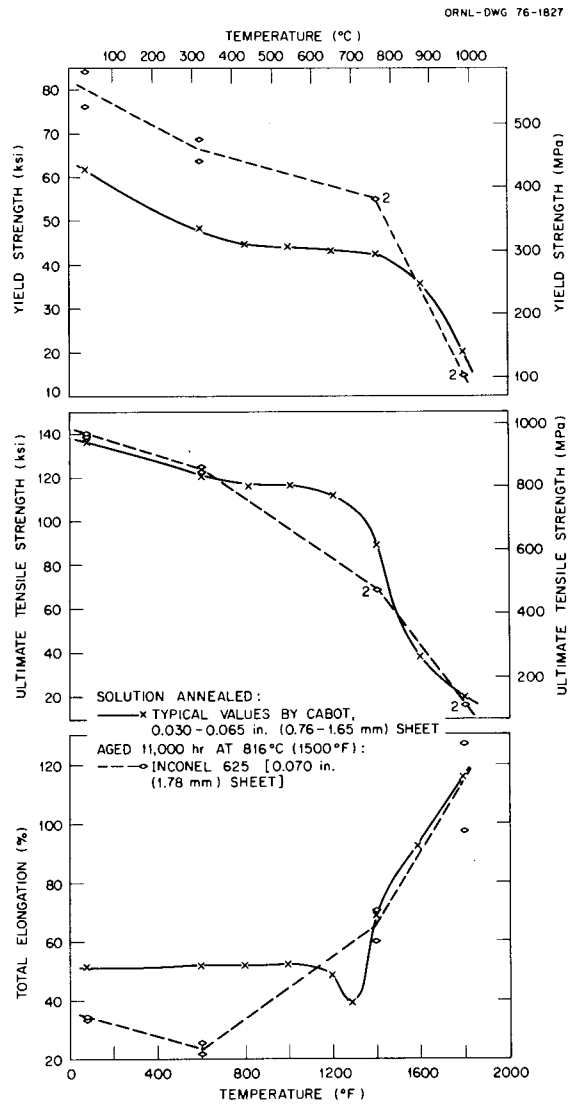

Fig. 4. Comparisons Between Effects of Solution Annealed and Aged Conditions on the Yield Strength, Ultimate Tensile Strength, and Total Elongation of Inconel 625.

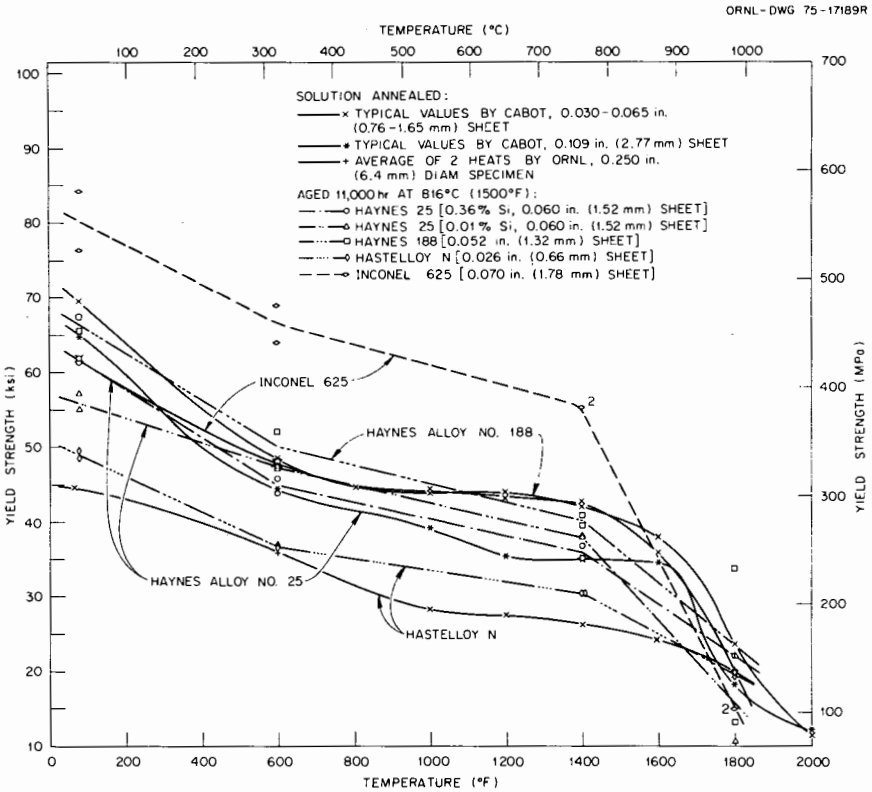

Fig. 5. Variation of Yield Strength with Test Temperature, All Alloys.

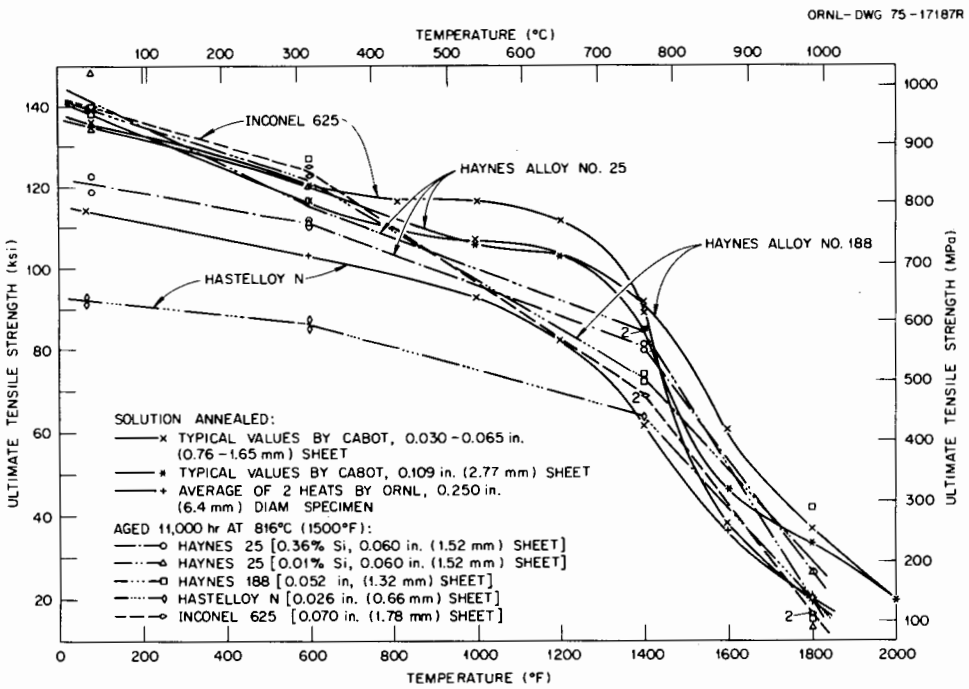

Fig. 6. Variation of Tensile Strength with Test Temperature, All Alloys.

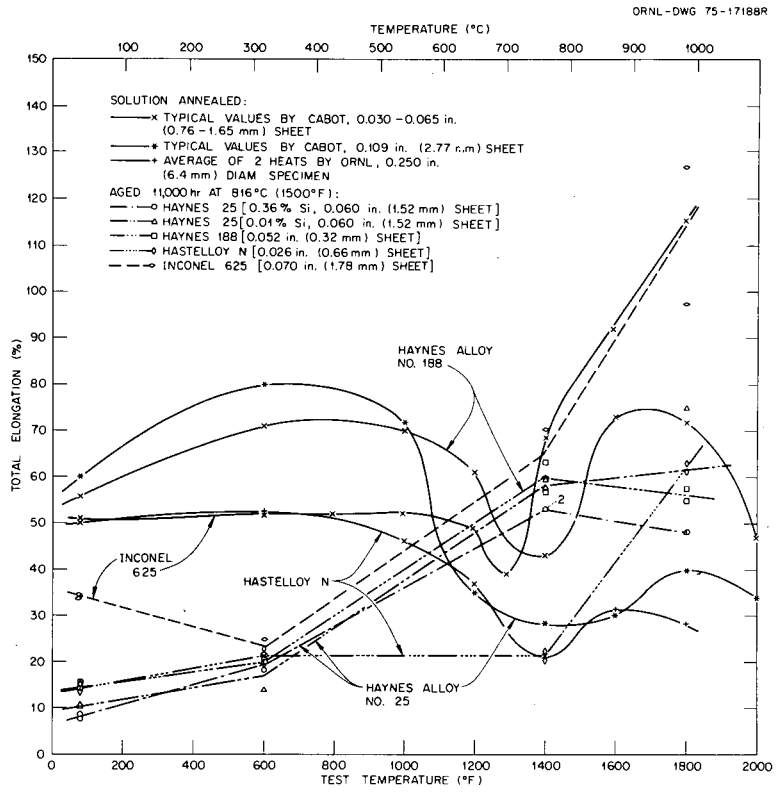

Fig. 7. Variation of Total Elongation with Test Temperature, All Alloys.

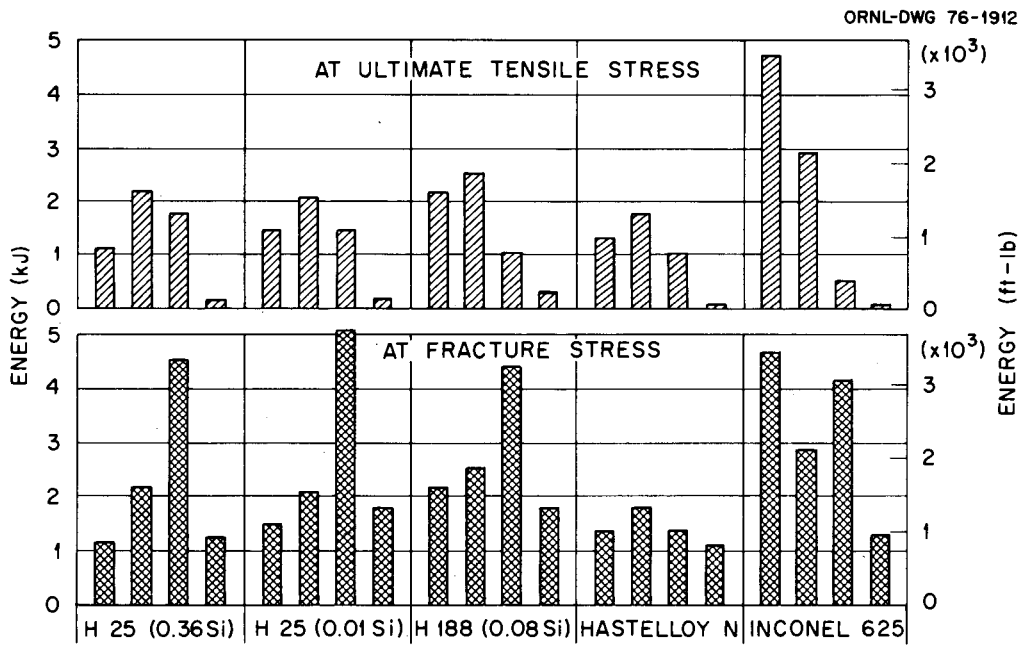

Fig. 8. Energy of Deformation at Ultimate Tensile and Fracture Stresses for Alloys Tested in Aged Condition. Bar charts for individual alloys give average of two values at 24, 316, 760, and 982°C (75, 600, 1400, and 1800°F), consecutively.

nearly as dramatic maxima in ductility were displayed for several of the alloys in the aged condition. This was unexpected and will be discussed later.

Figures 1 and 2 show numerous examples in which aging altered yield and tensile strength values of the cobalt-base alloys, although for the most part, these changes are relatively small and some may be within our experimental error.

It is informative to consider the combined effect of the yield and ultimate strengths along with total elongation from the toughness aspect. For example, the ductility maxima displayed by the aged cobalt-base alloys and Inconel 625 at 760°C are all the more significant when it is considered that at this temperature both tensile strength and yield strength are quite high. Yield strengths in the solution annealed state do not drop off substantially until some 100°C higher for these materials. This suggests high toughness for these aged alloys when tested at this temperature, and, indeed, the energies of deformation at fracture displayed in the bar charts of Fig. 8 show this.

The highest energy of deformation exhibited by any of the aged superalloys is the 5.1 kJ shown for 0.01%-Si Haynes alloy 25 at 760°C, the temperature of its ductility maximum. On the other hand, as noted earlier, aged Inconel 625 showed by far the best energy of fracture of all alloys at room temperature, and this energy also proved to be its best for all test temperatures.

Interestingly, the energies at ultimate stress and fracture stress are virtually the same for the 24 and 315°C tests in the cases of all the alloys (see Fig. 8). The reason for this is that the ultimate and fracture strengths at these low temperatures usually coincided (see Table 2), a situation perhaps characteristic of the overaged condition at low temperatures. Further, the patterns of energy change with test temperature for the three cobalt-base alloys are about the same, reflecting a similarity in their metallurgy. The patterns for the two nickel-base alloys, on the other hand, are quite different.

Metallographic and Electron-Beam Scanning Examinations

The Haynes alloys 25 and 188 are cobalt-base alloys that obtain their elevated-temperature strength by solid solution strengthening (contain around 14% W) and age hardening. Each has a carbide dispersion ($M_{23}C_6$ for Haynes 25 and M_6C for Haynes 188) for preventing excessive grain growth during heat treatment.[3,4] The Haynes alloy 25 is reported[3] to precipitate the M_7C_3, $M_{23}C_6$, and M_6C carbides and the Laves Co_2W and μ-Co_7W_6 phases in the order listed on aging at 815°C (our aging temperature);

---

[3]N. Yukawa and K. Sato, "The Correlation Between Microstructure and Stress Rupture Properties of a Co-Cr-Ni-W (HS-25) Alloy," *Trans. Japan Inst. Metals* 9(Supplement): 680–86 (1968).

[4]R. B. Herchenroeder, R. J. Matthews, J. W. Tackett, and S. J. Wlodek, "Haynes Alloy No. 188," *Cobalt* 54: 3–13 (March 1972).

and Haynes alloy 188 the M_6C, $M_{23}C_6$ and, Laves Co_2W in this order.[4] Yukawa[3] attributes age hardening in the former alloy at 815°C to the $M_{23}C_6$, M_6C, and Laves Co_2W phases.

The nickel-base alloys Hastelloy N and Inconel 625 also are solution strengthened by refractory metal additions, 16.5% Mo in the former and 9% Mo plus 3.5% (Nb + Ta) in the latter. No intermetallic compounds have been identified in Hastelloy N, but carbides precipitate and cause modest changes in properties.[5,6] Inconel 625 uses small additions of titanium and aluminum as deoxidants and grain refiners. Although this alloy is not ordinarily prescribed in the age-hardened condition, many precipitates have been identified in it.[7] As will be noted from our study subsequently, aging at 815°C promoted a substantial increase in yield strength from 24 to 760°C. Carbides of the MC type [Ti(N,C) and Nb(C,N)] are present in Inconel 625 as solution annealed, and M_6C and the phases γ^*, δ, and μ precipitate on aging at 760°C.[7]

As mentioned earlier, the metallographic and electron-beam scanning studies were directed mainly at specimens pulled at 24 and 760°C to explain contrasting behavior. In general, these methods of analysis revealed the fractures in the alloys tested at 760°C to be predominantly transgranular and ductile. The exception to this was Hastelloy N, which contained a massive, nearly continuous, precipitate concentrated largely in grain boundaries. At room temperature, where, with the exception of Inconel 625, all the alloys exhibited comparatively low ductility, failures were generally intergranular and brittle. Inconel 625, which gave the highest ductility of all the aged alloys at all test temperatures, exhibited transgranular and ductile-appearing fractures (see Table 2 for tensile properties).

The microstructures of the cobalt-base alloys in the solution annealed and aged conditions are illustrated in Figs. 9 and 10, respectively. The solution annealed and aged microstructures for Hastelloy N are shown in Fig. 11, while those for Inconel 625 are given in Fig. 12. The photographs for the aged condition were taken of the specimens pulled at room temperature at their fracture surface to show the characteristics of fracture at this temperature. All fields of view are in the plane of the specimen, and arrows in the applicable photomicrographs indicate direction of principal stressing.

Observe in Fig. 10 that failures in the aged cobalt-base alloy specimens tested at 24°C are predominantly intergranular, a finding confirmed for the 0.36% Si Haynes alloy 25 by scanning electron microscopy. This

---

[5]H. E. McCoy and R. E. Gehlbach, "Influence of Irradiation Temperature on the Creep-Rupture Properties of Hastelloy N," *Nucl. Technol.* 11(1): 45–60 (May 1971).

[6]H. E. McCoy, Jr., *An Evaluation of the Molten-Salt Reactor Experiment Hastelloy N Surveillance Specimens — Fourth Group*, ORNL-TM-3063 (March 1971).

[7]O. F. Kimball, W. R. Tieren, and D. R. Robert, *Effect of Elevated-Temperature Aging on the Mechanical Properties and Ductility of Ni-Cr-Mo-Cb Alloy 625*, GULF-GA-A-126831 (Oct. 1, 1973).

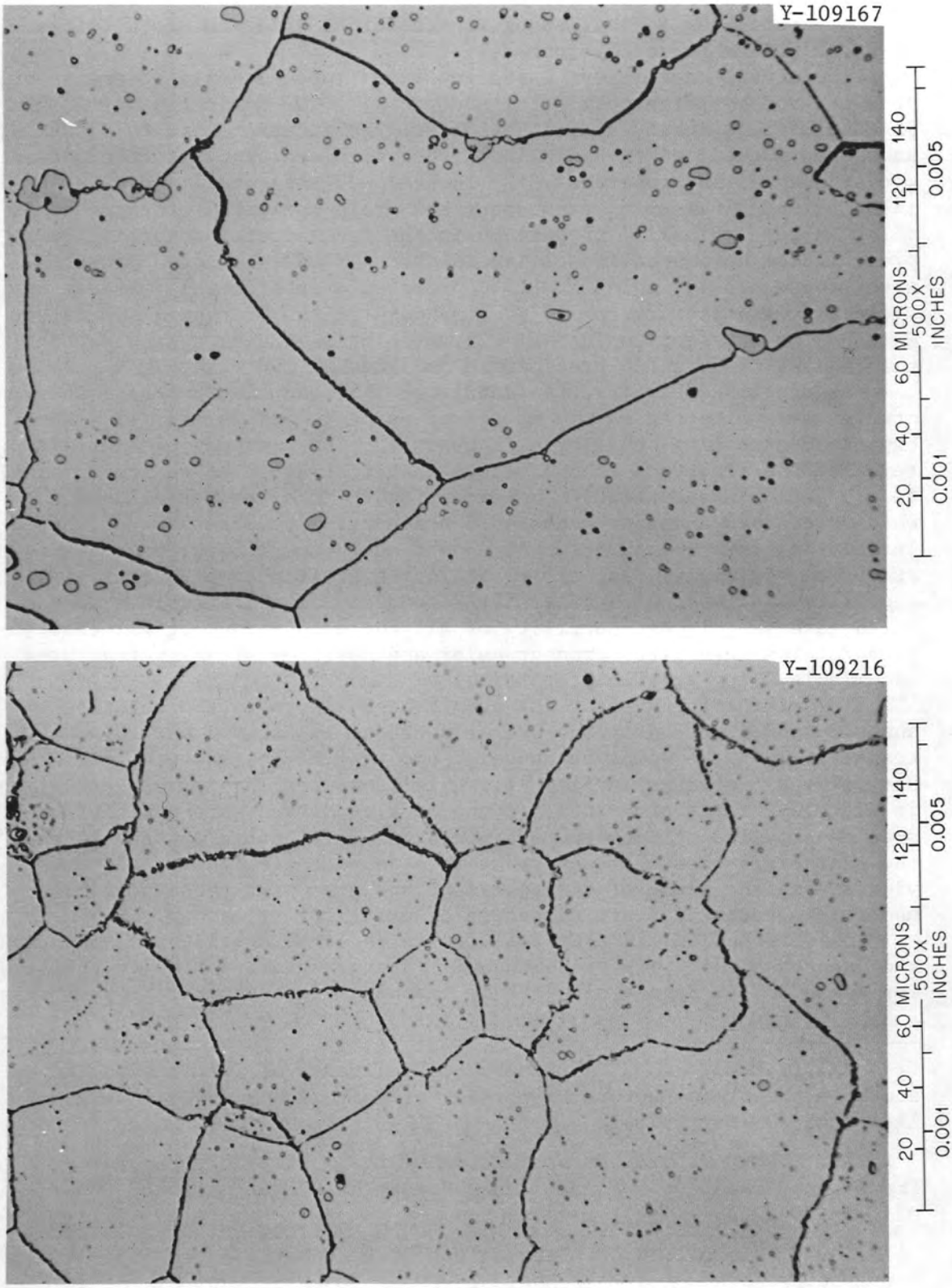

Fig. 9. Microstructures of Typical Haynes Alloys 25 (top) and 188 (bottom) in the Solution Annealed Condition. Etchant: glyceria regia.

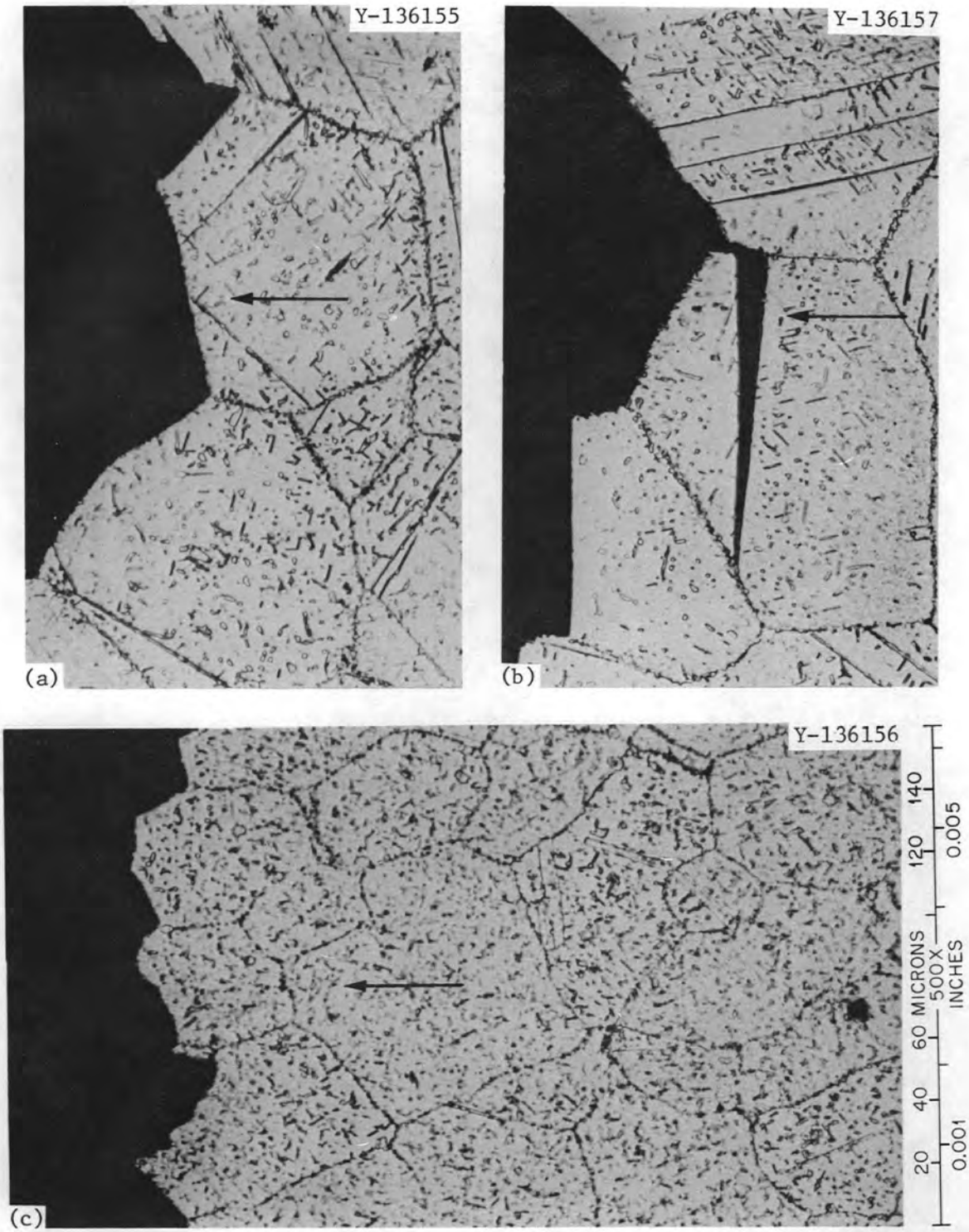

Fig. 10. Microstructures of Aged Cobalt-Base Alloys at Fracture Surface After Pulling to Failure at 24°C. Etchant: glyceria regia. Arrows indicate direction of principal stress. (a) Haynes alloy 25 (0.1% Si). (b) Haynes alloy 25 (0.36% Si). (c) Haynes alloy 188 (0.08% Si).

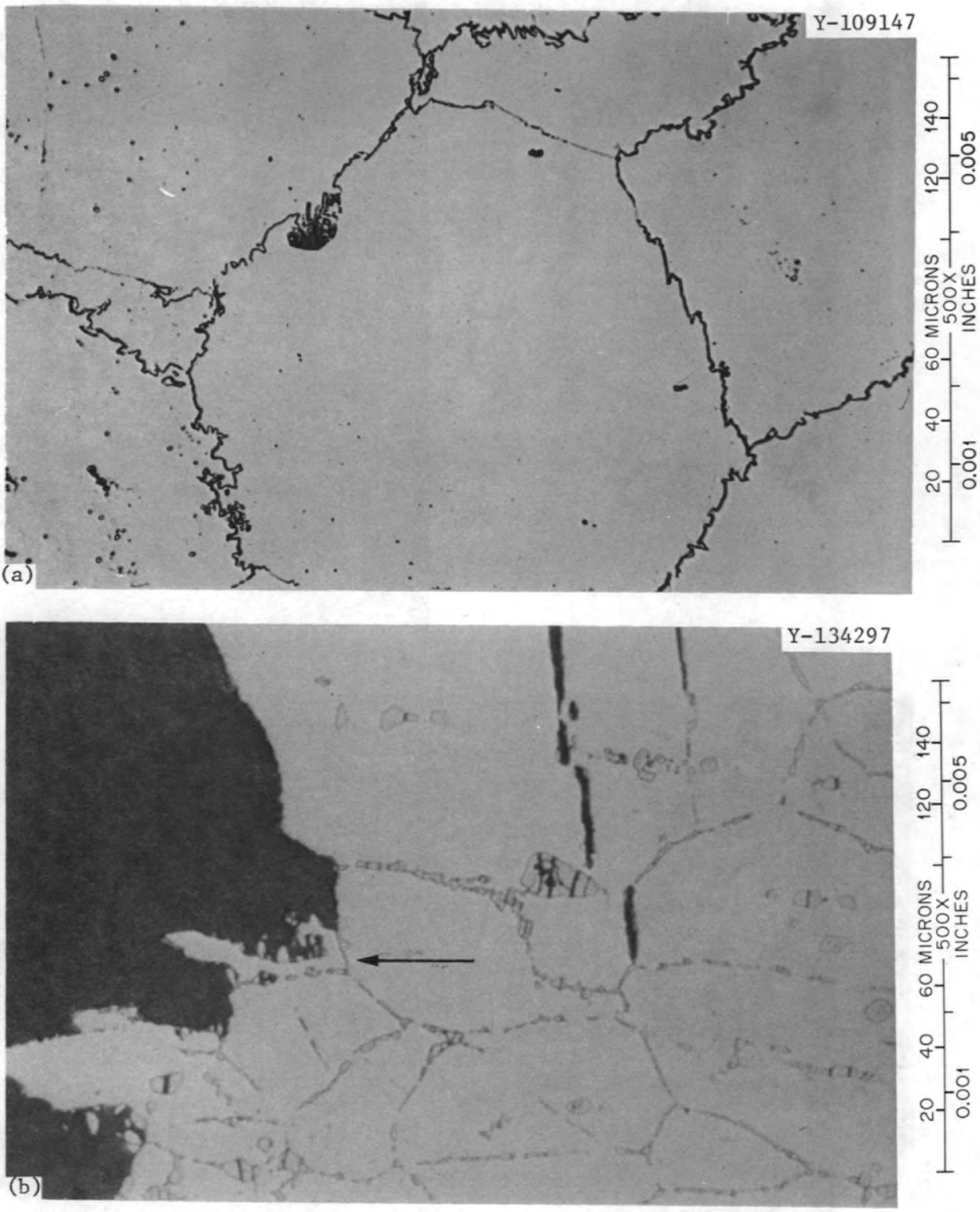

Fig. 11. Microstructure of Hastelloy N. Etchant: glyceria regia. (a) Solution annealed. (b) Aged 11,000 hr at 815°C and pulled to failure at 24°C. Arrow indicates direction of principal stress.

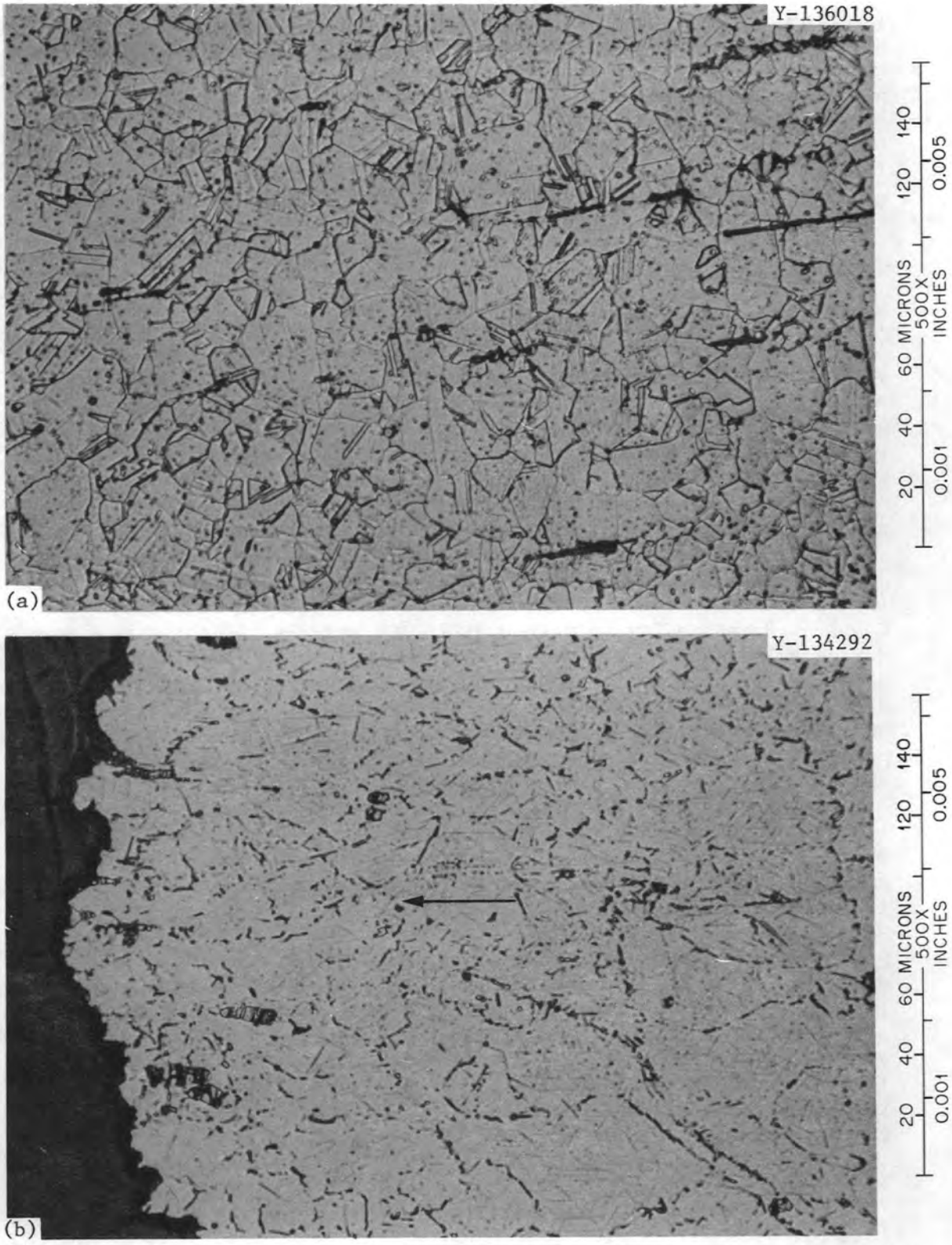

Fig. 12. Microstructure of Inconel 625. Etchant: glyceria regia. (a) Solution annealed. (b) Aged 11,000 hr at 815°C and pulled to failure at 24°C. Arrow indicates direction of principal stress.

was true although the precipitates in grain boundaries were semicontinuous. Moreover, a substantial portion of the within-grains precipitates in the two Haynes alloy 25 compositions was along low-index (Widmanstätten) planes or twin boundaries, providing semicontinuous and sometimes continuous paths across grains. Cracking appeared to have initiated in precipitates at twin boundaries and then proceeded largely intergranularly. The Haynes alloy 188 exhibited semicontinuous precipitates in grain boundaries and well distributed, disconnected particles within grains [Fig. 10(c)]. The amount of precipitates in the two Haynes alloy 25 compositions appeared to be about equal and that in Haynes alloy 188 slightly higher.

Failures in the Hastelloy N specimens tested at 24°C were basically intergranular (Fig. 11), in agreement with the precipitate being arrayed in massive and nearly continuous form in grain boundaries. The fractures in Inconel 625 tested at 24°C were just as decidedly transgranular in mode as the former alloy was intergranular and correlated with its precipitate being largely distributed within grains as a fine dispersion of discontinuous platelets (Fig. 12). The grain structure of Inconel 625 was comparatively fine.

The fractures in the specimens pulled at 760°C, which were transgranular except for Hastelloy N, displayed a number of interesting features. Figure 13 shows at high magnification the fracture surface of the 0.01% Si Haynes alloy 25 (top) and crack openings just adjoining the fracture (bottom). Figure 14 shows the fracture surface of the 0.36% Si Haynes alloy 25 tested at 760°C, and Fig. 15 the same for Haynes alloy 188. Observe that the fracture in each of the cobalt-base alloys is predominantly transgranular, an observation confirmed for the 0.36% Si Haynes alloy 25 by scanning electron microscopy. Cracks apparently initiated inside the precipitates (Fig. 13) and generally propagated across grains normal to the principal stress (Figs. 13 and 15).

Figure 16 shows the fracture surface of Hastelloy N pulled at 760°C. Although cracking was intergranular and, like at room temperature, progressed mainly along the massive grain boundary constituent, short, arrested cracks also formed across the constituent where it was aligned in the principal stress axis.

Finally, Fig. 17 shows the fracture surface of the Inconel 625 pulled at 760°C (top) and many small, well-distributed holes that developed in it at distances as far removed from the fracture as 6 mm (1/4 in.) (bottom). Cracking here, like for this alloy at room temperature, was transgranular and apparently originated within or at the ends of the Ti(N,C) and Nb(C,N) inclusions[8] so prevalent in Inconel 625 (Fig. 17). That the Inconel 625 was highly ductile in the aged condition (65% total elongation at 760°C and 114% at 980°C) accounts for the extensive dispersion of small holes that were able to develop at the

---

[8]These inclusions originate with founding Inconel 625 and are discernible by their characteristic yellow to orange [Ti(N,C)] and lavender-gray [Nb(C,N)] colors in the unetched microstructure, as reported by Kimball et al., GULF-GA-A-12683 (Oct. 1, 1973).

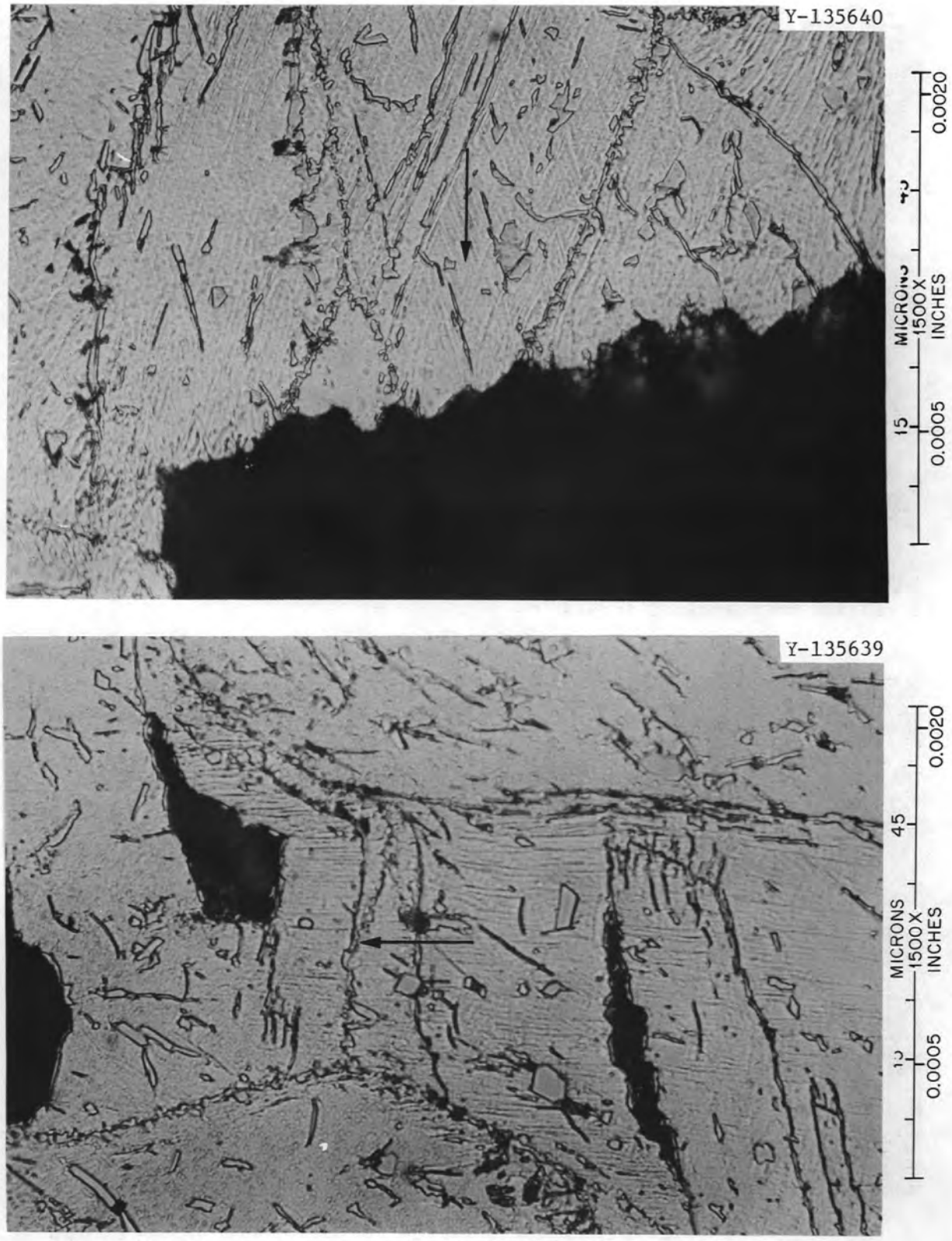

Fig. 13. Fracture Surface (top) and Crack Openings (bottom) in 0.01% Si Haynes Alloy 25 Specimen Pulled at 760°C. Etchant: 100 ml HCl + 12 drops H_2O_2. Arrows indicate direction of principal stress.

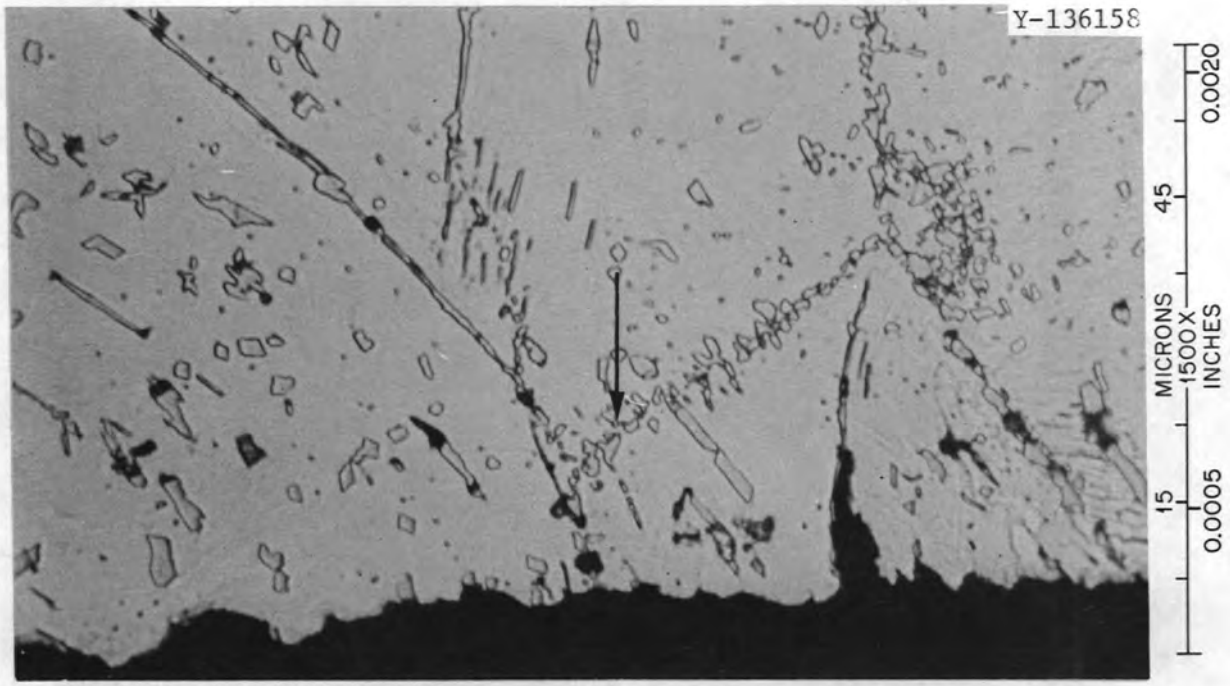

Fig. 14. Fracture Surface of 0.36% Si Haynes Alloy 25 Specimen Pulled at 760°C. Etchant: 100 ml HCl + 12 drops H_2O_2. Arrow indicates direction of principal stress.

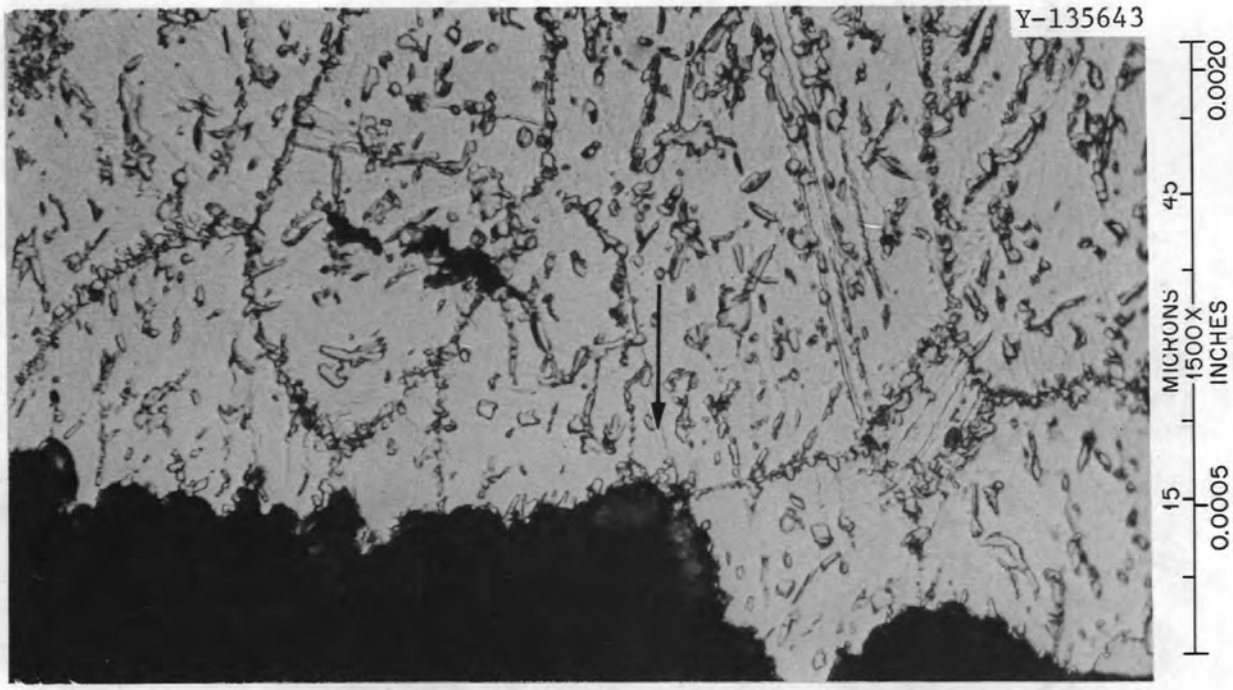

Fig. 15. Fracture Surface of Haynes Alloy 188 Specimen Pulled at 760°C. Etchant: 100 ml HCl + 12 drops H_2O_2. Arrow indicates direction of principal stress.

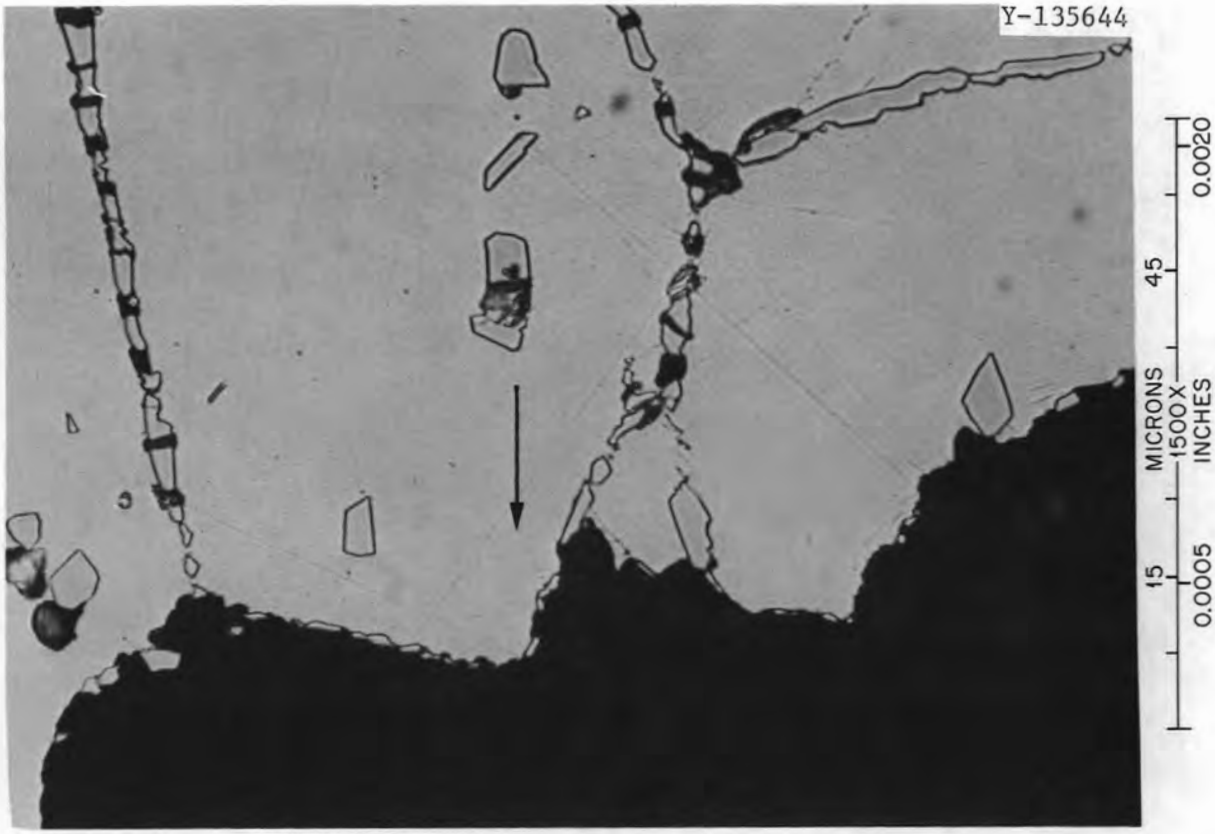

Fig. 16. Fracture Surface of Hastelloy N Specimen Pulled at 760°C. Etchant: 95 parts HCl — 5 parts. H_2SO_4 — 3 parts HNO_3. Arrow indicates direction of principal stress.

inclusions before rupture. Interestingly, one of the specimens ruptured at 980°C did so only after the stress had returned to the zero level, giving a fracture strength of like magnitude (see Table 2).

The results of the examinations made of fracture surfaces by scanning electron microscopy corroberated findings obtained by optical microscopy. Scanning electron micrographs of the fractures resulting from the 24 and 760°C tests in the 0.36% Si Haynes alloy 25 and Inconel 625 are illustrated in Figs. 18 and 19, respectively. The Haynes alloy 25 fractured predominantly at grain boundaries at 24°C (Fig. 18, top) and apparently through grains at 760°C (Fig. 18, bottom). The fracture surface developed by pulling at 760°C showed an abundance of the cup-and-cone feature commonly associated with ductility, whereas the surface developed at 24°C displayed little if any evidence of plasticity. The flat regions in the former micrographs (failure at 760°C) probably correspond to precipitate-laden twin boundaries, while the rough texture seen on some of the facets in the latter (failure at 24°C, 3000×) possibly are fragments of the grain boundary precipitates.

The scanning electron micrographs taken of the fracture surfaces of Inconel 625 at 24 and 760°C indicated transgranular fracture and, more significant, highly irregular and ligamented topology (Fig. 19), reflecting the high degree of ductility this alloy manifested in tests at 24, 760, and 980°C.

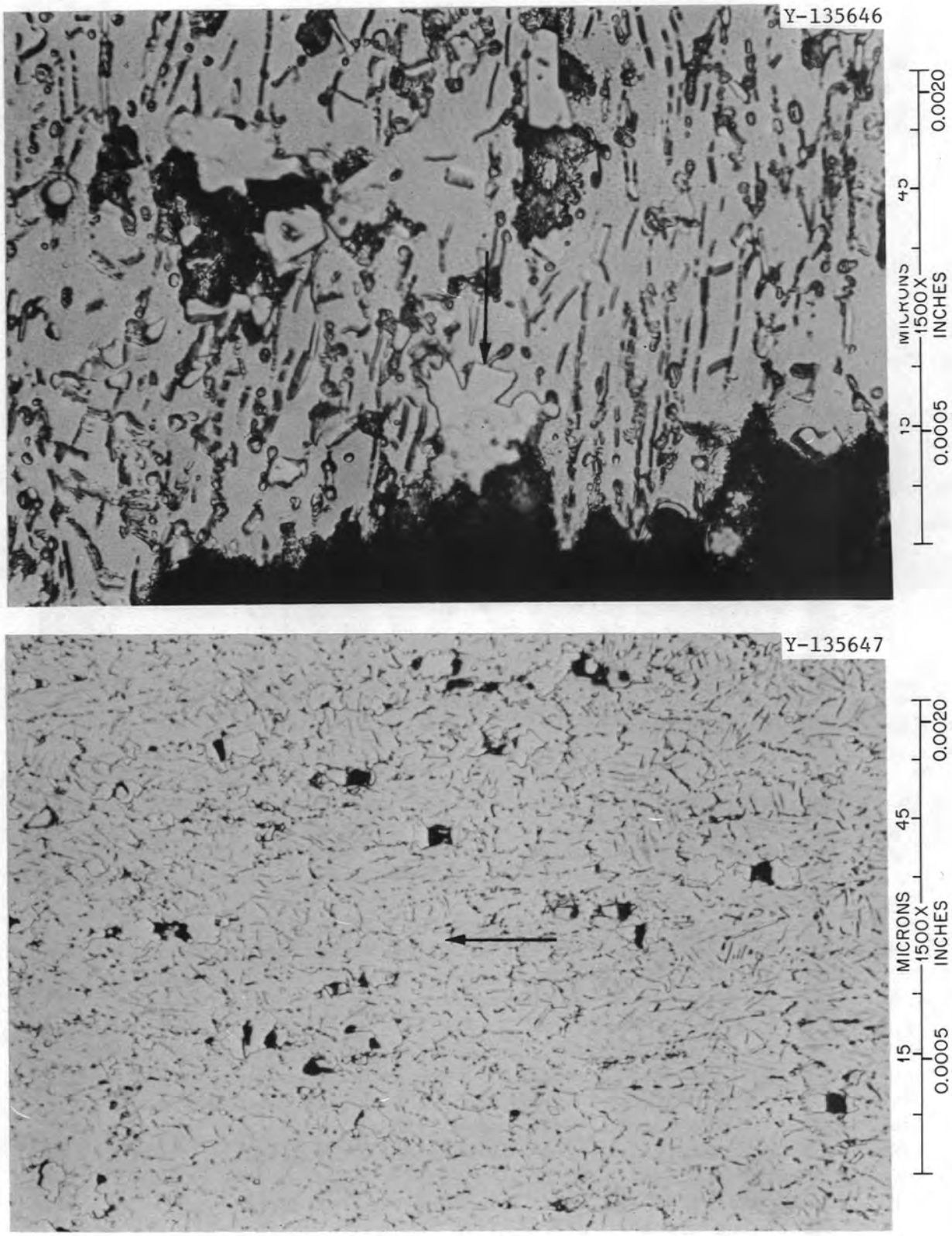

Fig. 17. Fracture Surface (top) and Small Holes (bottom) Developed in Inconel 625 Specimen Pulled at 760°C. Etchant: 10% oxalic acid in H_2O. Arrows indicate direction of principal stress.

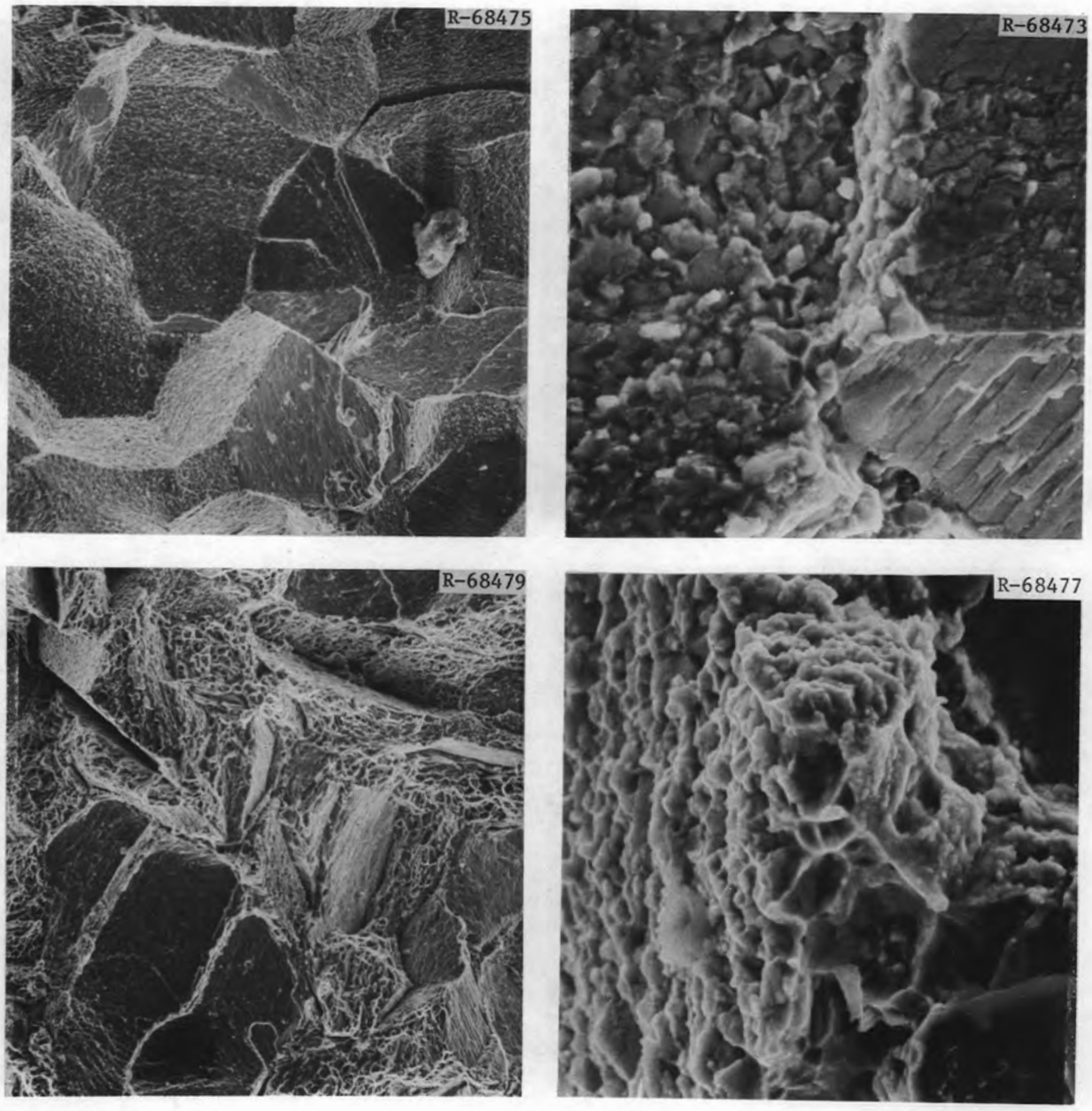

Fig. 18. Scanning Electron Micrographs of Haynes Alloy 25 (0.36% Si) at Fracture Surface after Pulling at Room Temperature (top) and 760°C (bottom). Left, 300×. Right, 3000×. Reduced 14%.

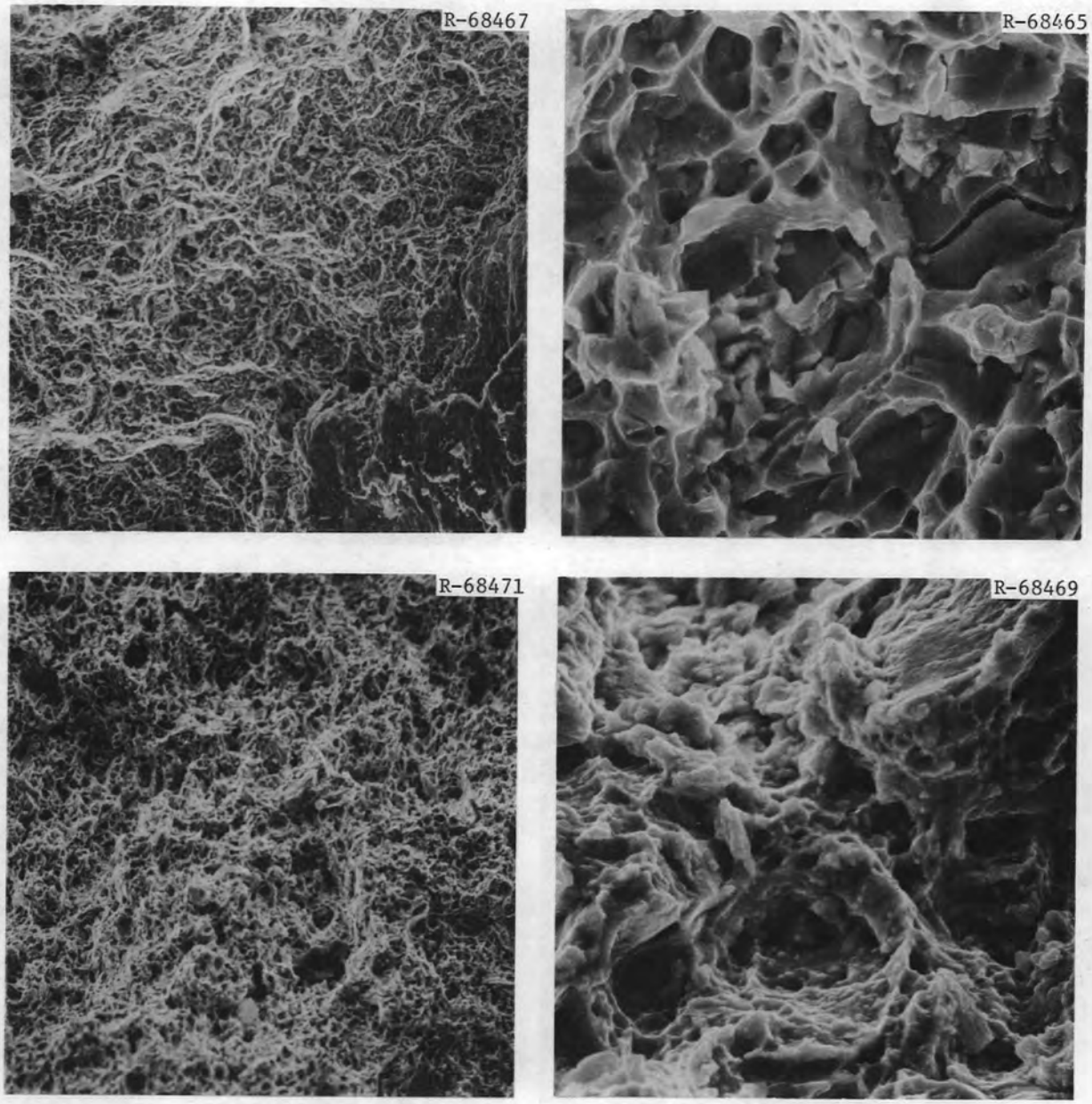

Fig. 19. Scanning Electron Micrographs of Inconel 625 at Fracture Surface after Pulling at Room Temperature (top) and 760°C (bottom). Left, 300×. Right, 3000×. Reduced 14%.

Phase Identifications

The identifications by x-ray diffraction made on residues extracted by electrolysis from samples of the alloys aged 11,000 hr at 815°C are given in Table 3. Since the Laves Co_2W phase is prominent in the precipitates of the Haynes alloys 25 and 188, the aging process was evidently well along. Calculations based on the weight of the extract, in relation to the amount of sample digested in making the separations, indicated that the aged 0.36% Si Haynes alloy 25 contained 14.5% precipitate, the aged 0.01% Si Haynes alloy 25 14.8%, and so on. By approximate calculations based on the assumption that the precipitates in the Haynes alloys consisted wholely of Laves Co_2W phase, the aging would have depleted their matrix of over 50% of the tungsten content. By a similar calculation, aging would have depleted the matrix of Hastelloy N of 21% of its molybdenum content. However, these calculations assumed that the original carbide dispersions contained in these alloys for retarding grain growth did not contain appreciable amounts of the heavy metal hardeners. A subsequent check with an electron beam microprobe analyzer indicated that the latter assumption was not justified, and consequently further study was made of the distribution of tungsten within the aged 0.36% Si Haynes alloy 25 with the microprobe analyzer.

Table 3. X-Ray Diffraction Examination of Residues

Alloy	Phases (Intensity)	Amount (wt %)
Haynes 25 (0.36% Si)	Laves Co_2W(Strong); 4 lines[a](Strong)	14.5
Haynes 25 (0.01% Si)	Not examined	14.8
Haynes 188	Laves Co_2W(Very Strong); 2 lines[a](Medium)	15.2
Hastelloy N	Mo_6Ni_6C	5.0

[a]Did not correspond to any of the carbide phases previously reported for this alloy.

Figure 20 shows electron-beam scanning images from the microprobe of the aged Haynes alloy 25. The top picture is a backscattered electron image and the bottom picture is an x-ray display showing the distribution of tungsten. Similarly, Fig. 21 gives the same information on this alloy in the solution annealed condition. Tungsten obviously concentrated heavily in this aged alloy but it also resided rather heavily in the original carbide particles as well.

Using pure tungsten metal as a standard, semiquantitative microprobe analyses conducted in sequence on the annealed and aged matrices

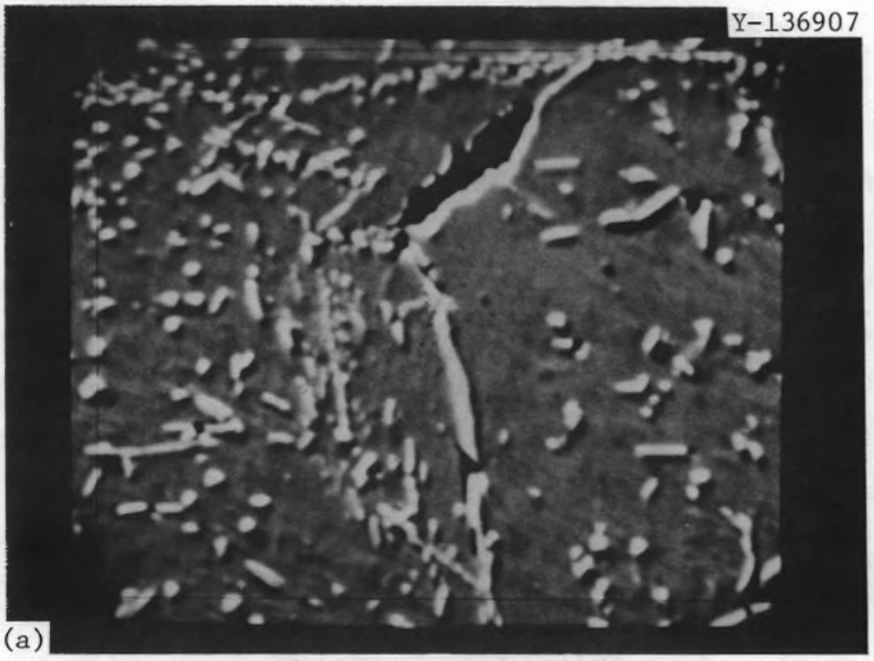

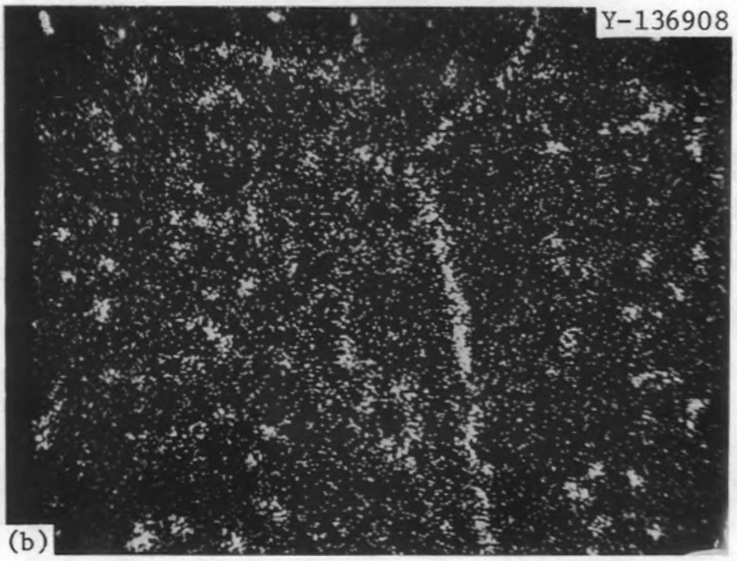

Fig. 20. Electron-Beam Scanning Images of Overaged 0.36% Si Haynes Alloy 25 (11,000 hr at 815°C). 1500×. (a) Backscattered electrons. (b) Tungsten Mα x-ray display. Rift at top of image is a crack.

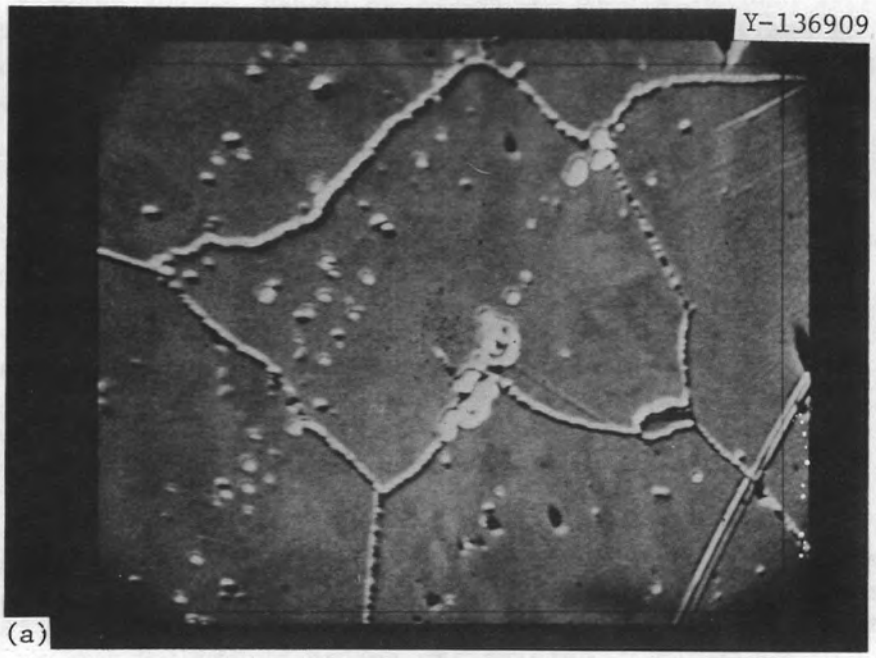

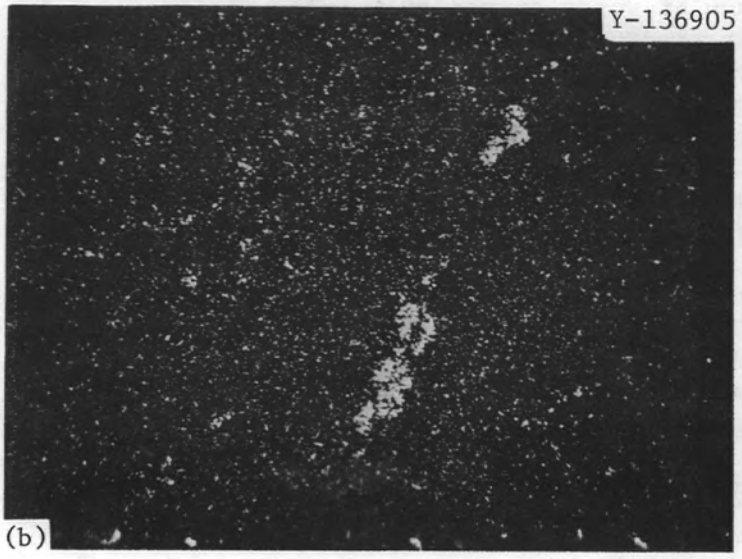

Fig. 21. Electron-Beam Scanning Images of Solution Annealed 14.5% W Haynes Alloy 25 (1 hr at 1150°C). 500×. (a) Backscattered electrons. (b) Tungsten Mα x-ray display.

indicated that the long-term aging depleted the tungsten concentration in the matrix by only about 33%. Further, step scans conducted of the matrix between precipitated particles revealed an even distribution of tungsten within the limits of detection of the microprobe. Tungsten was not as heavily concentrated in the original carbide particles as in the aging-induced precipitates but was a major constituent element.

DISCUSSION OF RESULTS

A most significant finding of the present work was the very high tensile ductilities and toughnesses displayed by the aged superalloys at 760°C, a temperature just 55°C below where they had been subjected to prolonged aging to determine the effects of embrittling phases. The 760°C temperature was selected as one of the four test temperatures because it was generally regarded as a temperature at which superalloys in the solution annealed condition exhibit a pronounced dip in ductility, and it was of interest in particular to note properties of aged alloys at this temperature.

According to the Rhines and Wray model,[9–11] all ductile metals and alloys should show a ductility minimum at elevated temperature. They postulate that at low temperatures fracture occurs by the usual transgranular crack propagation mechanism and ductility is high. At temperatures near the minimum, deformation occurs by grain boundary shear. The intergranular voids formed at triple points grow unhindered, causing intergranular fracture with drastic loss in ductility. At high temperatures, recrystallization occurs simultaneously with intergranular void formation, continuously breaking up the intergranular fracture path. As a result, ductility increases again.

Our earlier illustrated ductility curves (Fig. 7) which included data for the solution annealed and aged conditions, are reproduced in Fig. 22 with information on mode of fracture incorporated. Information on cracking mode for the aged condition described earlier and that predicted by the Rhines model[9–11] for the solution annealed condition are used. The fracture mode at 980°C of Inconel 625 was transgranular, and, while the mode was not examined for all aged alloys at this temperature, it would be expected to be predominantly transgranular as long as the test temperature does not too closely approach melting.

Observe from the graph the dramatic reversal in the ductility response between the solution annealed and overaged conditions. Insofar as the author knows, this had not been previously cited. It appears

---

[9]F. N. Rhines and P. J. Wray, "Investigation of the Intermediate Temperature Ductility Minimum in Metals," *Trans. Am. Soc. Met.* 54: 117–28 (1961).

[10]E. Shapiro and G. E. Dieter, "Fracture and Ductility in Hot Torsion of Nickel," *Metall. Trans.* 2: 1385–91 (1971).

[11]E. Shapiro and G. E. Dieter, "High Temperature-High Strain Rate Fracture of Inconel 600," *Metall. Trans.* 1: 1711–19 (1970).

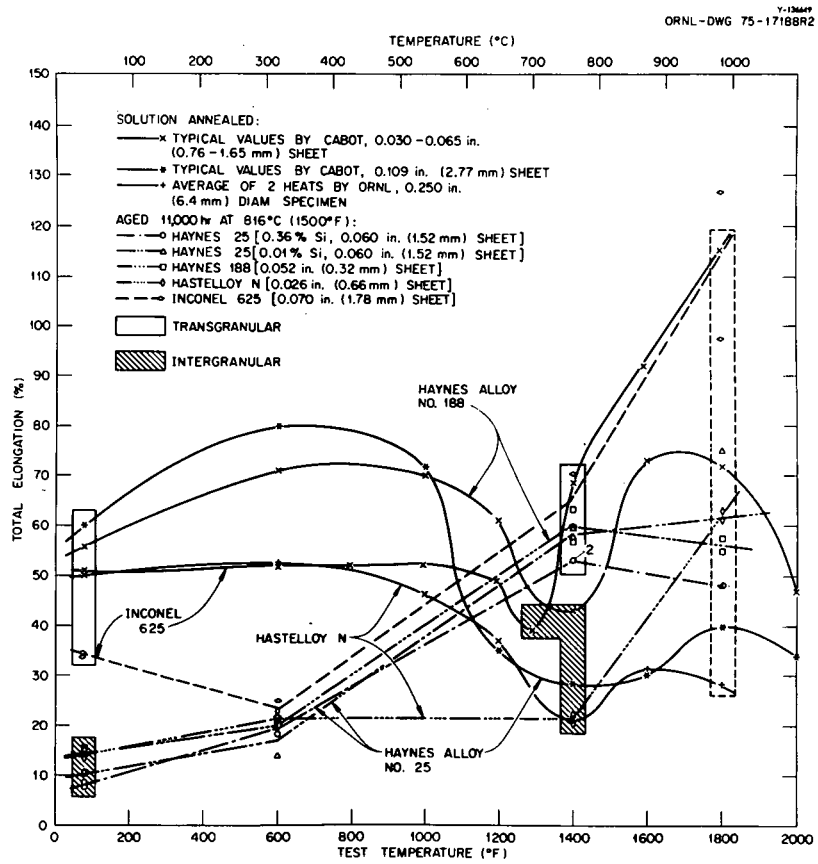

Fig. 22. Correlation of Ductility Response with Fracture Mode.

that the ductility minimum of cobalt-base alloys centers at 760°C (1400°F) and that of nickel-base material at around 700°C (1300°F). Arkoosh and Feore[12] obtained a minimum at 677°C (1250°F) for Hastelloy X.

Note in Fig. 22 that high ductility apparently equates with transgranular fracture and low with intergranular. All the overaged superalloys except Inconel 625 showed intergranular failure and very low ductility at room temperature. At 760°C all overaged alloys displayed transgranular failure and very high ductility except Hastelloy N. That the aged alloys behaved as they did at room temperature is explainable by their individual microstructures. All had moderate to high amounts of embrittling phases arrayed semicontinuously to nearly continuously in their grain boundaries except for ductile Inconel 625, whose grain boundary constituents could be described as low in amount, fine, and discontinuous. Since the microstructures described for the aged specimens tested at room temperature surely must have prevailed for those pulled at 760°C, the underlying reasons for the highly ductile responses

[12]M. A. Arkoosh and N. F. Feore, "Elevated Temperature Ductility Minimum in Hastelloy Alloy X," *Metall. Trans.* 3: 2235–40 (August 1972).

experienced at 760°C must be ascribed to additional factors. That aged Inconel 625 was ductile at 760°C, however, was no surprise in view of its favorable microstructure and good ductility at room temperature. Aged Hastelloy N contained a massive, almost continuous carbide precipitate in its grain boundaries, and that it continued to be rather brittle (intergranular failure mode) to 760°C also was no surprise. Thus, the very high ductility obtained for the aged cobalt-base alloys at 760°C, a temperature clearly coinciding with the ductility minimum of this group of alloys as solution annealed (Fig. 22) remains to be explained.

It should be recognized, first, that an important effect contributing to the minimum ductility phenomenon in superalloys probably was not operative for the present aged alloys. This is the rapid precipitation of carbides at grain boundaries and along deformation bands as the material is plastically deformed at the minimum temperature. Nor would it be expected for the present alloys to have sensitized (formed shallow continuous precipitates at grain boundaries) incident to heating up to the 760°C test temperature. These particular effects are not likely since, as was shown earlier, the prior aging at 815°C had approached completion and the matrix probably had virtually spent its capacity for further precipitation. This reasoning helps explain the absence of a minimum but does not account for why the factors that had caused embrittlement at room temperature did not do so at 760°C.

It would appear that the tungsten depletion effect observed in the aged cobalt-base alloys may have an important bearing. Another factor may be the relative fragility of the precipitates at high temperature compared with low; that is, the Laves Co_2W phase may begin to show some degree of toughness at the miminum temperature. The means whereby tungsten depletion might contribute would be for it to impart a higher plasticity to the matrix so as to thwart crack propagation once it initiates in the precipitates. Since tungsten in these alloys is the primary contributor to strength at high temperatures, the chromium plus diminished tungsten in solid solution may well provide high hardness at room temperature but a substantially more plastic matrix at 760°C.

Although the molybdenum distribution in aged Hastelloy N was not examined by electron-probe analysis, assessment by the phase extraction technique indicated that depletion of molybdenum from its matrix by precipitation of Mo_6Ni_6C was not great. Interestingly, Hastelloy N was the only alloy examined not to exhibit the reversal effect. The Mo_6Ni_6C phase, incidentally, had not been previously reported in Hastelloy N.

The high energies of fracture exhibited by the aged cobalt-base alloys at 760°C could offer practical advantages in their application as containment for isotopic power conversion units. For toughness in the temperature range from 24 to 316°C, aged Inconel 625 would be favored over the cobalt-base alloys. The extent to which the toughness advantages of these materials hold up under accelerated conditions of test is worthy of determination. Testing under impact conditions such as the Charpy test is desirable.

It is important to recognize that the tensile properties described herein for these superalloys are for the condition of overaging at 815°C. Aging at lower temperatures or for shorter periods of time could lead to significantly different results.

SUMMARY AND CONCLUSIONS

Tensile tests were conducted at 24, 316, 760, and 982°C (75, 600, 1400, and 1800°F) on samples of two Haynes alloy 25 compositions (0.01 and 0.36% Si), Haynes alloy 188, Hastelloy N, and Inconel 625 that had been solution annealed and aged 11,000 hr at 815°C. The results of these tests were compared with typical tensile properties of the same alloys in the solution annealed condition. Energies of fracture (toughnesses) were established from the engineering stress-strain curves.

Long-term aging affected the total elongation in these materials much more than yield strength and ultimate tensile strength, which in turn, significantly influenced their toughness. At room temperature, the aging greatly reduced the ductility, whereas at 760°C the ductility was usually increased over the solution annealed values. The reduction in percent elongation of aged alloys at 24°C ranged from 33% (for Inconel 625) to as much as 86% (for 0.36% Si Haynes alloy 25). At 760°C, the total elongations ranged from 53% (for 0.36% Si Haynes alloy 25) to 65% (for Inconel 625), except in the case of Hastelloy N, which exhibited brittle fractures of relatively low ductility at both 760 and 24°C. At 760°C the high ductilities displayed by the cobalt-base alloys and Inconel 625 were responsible for very high toughness values, which for the cobalt-base alloys were 2 to 3 times higher than at the other test temperatures. Inconel 625 exhibited a fracture toughness at 24°C over twice that of the other alloys at this temperature.

The tensile properties, especially ductility and toughness, correlated with the mode of fracture and the amount, identity, and morphology of the precipitates. The relatively low ductility of Hastelloy N at 24 to 760°C was explained by intergranular fracture influenced by a massive, semicontinuous to continuous precipitate of Mo_6Ni_6C carbide in grain boundaries. Semicontinuous precipitates of brittle phases (largely Laves Co_2W) influenced intergranular fracture in the aged cobalt-base alloys at 24°C. At 760°C (generally the temperature of a ductility minimum for these alloys in the solution annealed condition) the fracture of the aged cobalt-base alloys and Inconel 625 was predominantly transgranular. The transgranular fracture and high ductility of Inconel 625 at 760°C (also at 24 and 982°C) were explained by the discontinuity and fineness of its precipitates, prevalent both in grain boundaries and grains. The silicon level in the Haynes alloy 25 did not significantly affect the aged microstructure, although a low silicon content appeared to slightly improve ductility and toughness. The transgranular fracture of the cobalt-base alloys at 760°C, whose mode at 760°C was different from that at 24°C in spite of ostensibly the same microstructure, was attributed to a substantial depletion of tungsten from the matrix, among other considerations.

High ductility and toughness in all the alloys, both solution annealed and overaged, were equated with transgranular fracture and low with intergranular.

ACKNOWLEDGMENTS

The author expresses sincere appreciation to Arnold Litman, Division of Nuclear Research and Applications, ERDA, whose foresight led to the present study, and to C. R. Brinkman (Group Leader) and A. C. Schaffhauser (Program Manager) for their aid. He is indebted to L. T. Ratcliff for conducting the tensile tests. Grateful acknowledgments are extended to C. W. Houck for conducting the metallographic work, to R. S. Crouse for doing the electron beam microscopy, to J. M. Leitnaker for performing analyses on electrolytically extracted phases, and to the ORNL Graphic Arts Department for preparing figures and to S. Peterson for editing and Judy Young for preparing the manuscript. Finally, the author acknowledges David Goslee, who prepared the test specimens and performed the aging treatments when at the Hittman Corporation.

ORNL-5174
UC-33 (Nuclear
Propulsion Systems
and Aerospace Safety)

INTERNAL DISTRIBUTION

1–2. Central Research Library
3. Document Reference Section
4–8. Laboratory Records Department
9. Laboratory Records, ORNL RC
10. ORNL Patent Office
11. D. N. Braski
12. C. R. Brinkman
13. D. A. Canonico
14. R. E. Clausing
15. J. H. DeVan
16. J. R. DiStefano
17. R. G. Donnelly
18. K. Farrell
19. G. M. Goodwin
20–29. J. P. Hammond
30. D. E. Harasyn
31. R. L. Heestand
32. R. F. Hibbs
33–35. M. R. Hill
36. H. Inouye
37. E. Lamb
38. C. T. Liu
39. W. R. Martin
40. H. E. McCoy
41. C. L. Ottinger
42. P. Patriarca
43. H. Postma
44. T. K. Roche
45–79. A. C. Schaffhauser
80. V. K. Sikka
81. G. M. Slaughter
82. J. O. Stiegler
83. R. W. Swindeman
84. D. B. Trauger
85. J. R. Weir, Jr.
86. C. L. White
87. R. O. Williams
88. Paul M. Brister (consultant)
89. John Moteff (consultant)
90. Hayne Palmour III (consultant)
91. J. W. Prados (consultant)
92. N. E. Promisel (consultant)
93. D. F. Stein (consultant)

EXTERNAL DISTRIBUTION

94. ERDA DIVISION OF NUCLEAR RESEARCH AND APPLICATION, Washington, DC 20545

    Assistant Director, Research Programs

95. ERDA OAK RIDGE OPERATIONS OFFICE, P.O. Box E, Oak Ridge, TN 37830

    Director, Research and Technical Support Division

96–243. ERDA TECHNICAL INFORMATION CENTER, Office of Information Services, P.O. Box 62, Oak Ridge, TN 37830

    For distribution as shown in TID-4500 Distribution Category, UC-33 (Nuclear Propulsion Systems and Aerospace Safety)

☆ U.S. GOVERNMENT PRINTING OFFICE: 1976-748-189/449